ISTITUTO ITALIANO
DI TECNOLOGIA

UNIVERSITÀ DEGLI STUDI
DI GENOVA

Università degli Studi di Genova

Corso di Dottorato in Neuroscienze

Curriculum Neuroscienze e Neurotecnologie

Ciclo XXXVI

"Sex hormones dependent modulation of thalamic inputs to striatal fast spiking interneurons"

Author: **Mariaelena Francesca Veggi**

Supervisor: **Raffaella Tonini**

Table of contents

Abstract

Growing evidence suggests that many striatal-mediated behaviors and relevant disorders are sensitive to biological sex and estrous cycle-dependent changes in sex hormones (*Meitzen et al., 2018*). Though striatal-related behaviors and pathologies display clear sex dimorphism, the mechanisms by which sex and gonadal hormones influence striatal neurons´ physiology remain largely unknown (M*eitzen et al., 2018*). Most of the works have focused on medium-sized GABAergic spiny projection neurons (SPNs also referred to as ‘‘medium spiny neurons’’) (*Burke et al., 2017*). Besides the direct action on SPNs through membrane and/or nuclear receptors, sex hormones have been proposed to act also on striatal interneurons, which synapse on SPNs (*Krentzel & Meitzen, 2018a*), thus shaping striatal network activity and behavioral outcome *(Barth et al., 2015; Meitzen, 2018; Krentzel., 2020; McArthur and Gillies, 2011; Chuhma et al., 2011*). The relationship between striatal interneurons and sex hormones has been investigated only at the behavioral level (*Krentzel & Meitzen, 2018*), indicating that specific disruption of fast-spiking interneuron (FSI) sub population in mice dorsal striatum is sufficient to produce autism spectrum disorder and Tourette syndrome-like behavioral abnormalities and aberrant signaling in SPNs activity in males but not in females (*Rapanelli et al., 2017*). FSIs exert a crucial position in intrastriatal information processing of inputs that are conveyed to the striatum mainly from the cortex and thalamus (*Hjorth et al., 2020*).

In this study, we combined ex vivo pharmacological and optogenetic approaches with fiber photometry to examine how sex and the estrous cycle influence FSI integration of thalamic inputs and intrinsic excitability. We found that FSIs responsiveness to thalamic inputs is affected by both sex and estrous cycle. Male FSIs showed a stronger integration of thalamic inputs compared to females, while in females, FSI interneuron thalamic input integration was affected by the estrous cycle stage. Thus, our investigation reveals evidence supporting a sex-dependent modulation of synaptic processing in striatal FSIs. Synaptic integration is a cellular process that underlies motor control and learning, therefore sex-dependent regulation of thalamic inputs on FSIs could have strong implications for striatal behavioral outputs. By further screening FSI physiology, we found that FSI intrinsic excitability was affected by sex and gonadal hormone levels throughout the estrous cycle.

Manipulating estrogen-mediated signaling exacerbated the excitability differences observed indicating a possible estradiol role in modulating FSI ionic conductances. These findings identify modulation of the thalamus-FSI microcircuit as one of the possible substrates for sex differences in striatal-based behavior and psychomotor disorders caused by striatal dysfunction.

Aims and relevance

The striatum constitutes the primary input structure of the basal ganglia (*Graybiel & Grafton, 2015*; *Jin and Costa, 2010*). By receiving major excitatory projections from the cortex and the thalamus, it mediates critical behavioral functions, which include motivated behavior, learning, and sensorimotor outcome (*Kreitzer and Malenka, 2008; Baez-Mendoza and Schultz, 2013; Palmiter., 2008; Graybiel and Grafton, 2015, Yin, 2010; Bradfield et al., 2013).* Consistent with these broad functions, striatal dysfunction contributes to a variety of diverse neurological and psychiatric diseases including Parkinson's disease, autism, schizophrenia, depression, and addiction (*Pickrell et al., 2011; Kuo and Liu, 2020; Di Carlo et al., 2019; Simpson et al., 2010; Epstein et al., 2006; Burke et al., 2017*).

Growing evidence suggests that many striatal-mediated behaviors and relevant disorders are sensitive to biological sex and fluctuations in sex steroid hormones (*Meitzen et al., 2018*), which include estradiol, the most potent estrogen, testosterone, the principal androgen, and progesterone, an essential progestin (*Thomas and Potter, 2012; Kloner et al., 2016; Stefaniak et al., 2023*).

In animal models, the relationship between sex hormones and striatal-related behaviors has mostly been studied in the context of locomotor and sensorimotor responsiveness (*Meitzen et al., 2018*), with female rats showing increased running-wheel and open-field locomotor activity, exploratory behavior, and sensory responsiveness (S*tudelska & Beatty, 1978*) compared to males. Sex differences in drug responsiveness have also been extensively investigated. Female rats show an enhanced rate of acquisition of psychostimulant self-administration and tend to escalate drug consumption more rapidly than males, recapitulating addiction traits in humans. Besides addiction, other striatal-mediated disorders emerge to be sex-biased in humans (*Meitzen et al., 2018*). For instance, differential incidence and phenotype between men and women have been reported in Tourette syndrome and aspect of autism spectrum disorder (*Rapanelli et al., 2017*), as well as in anxiety-related behaviors (*Nillni et al., 2011*), and movement disorders, such as dyskinesia (*Castrioto et al., 2010*). In Parkinson's disease (PD), sex is the strongest risk factor, as men are more prone to develop PD. Moreover, in PD female patients, symptoms´

severity and motor coordination have been associated with monthly changes in gonadal hormones (*Meitzen et al., 2018*).

Though striatal-related behaviors and pathologies display clear sex dimorphism, the mechanisms by which sex and gonadal hormones influence striatal neurons´ physiology remain largely unknown (M*eitzen et al., 2018*). Ninety-five percent of striatal neurons consist of medium-sized GABAergic spiny projection neurons (SPNs) (*Author et al., 1985*). They form the major striatal inputs and striatal-only outputs and are traditionally divided according to their projection targets and dopamine receptor expression (*Burke et al., 2017*). In rodents, SPNs do not exhibit anatomical nor morphological sex-dimorphism (*Wong et al., 2016*), but they do show differences in functional electrophysiological properties (*Wong et al., 2016*). Ex vivo, SPNs from female rats, exhibited increased intrinsic excitability compared to male SPNs, as shown by increased evoked action potential in response to excitatory current injection slope, hyperpolarized threshold, and decreased afterhyperpolarization magnitude. When recorded from gonadectomized males and females, differences in active properties were abolished, supporting the hypothesis that the presence of the estrous cycle was needed to induce sex differences in SPNs (*Dorris et al., 2015*). Besides the direct action on SPNs through membrane and/or nuclear receptors, sex hormones have been proposed to act also on striatal interneurons, which synapse on SPNs (*Krentzel & Meitzen, 2018a*), thus shaping striatal network activity and behavioral outcome (*Barth et al., 2015; Meitzen, 2018; Krentzel., 2020; McArthur and Gillies, 2011; Chuhma et al., 2011*).

The remaining 5% of striatal neurons consist of several populations of interneurons that have been classified based on their intrinsic electrophysiological properties, neurochemical, and/ or molecular expression profiles. The relationship between striatal interneurons and sex hormones has been investigated only from a behavioral point of view (*Krentzel & Meitzen, 2018*), in the context of autism spectrum disorder (ASD) and Tourette syndrome (TS). Both pathologies are sex-biased, being more common in males than females (Redfield et al., 2014). FSIs' specific disruption in mice dorsal striatum emerged sufficient to produce ASD and TS-like behavioral abnormalities in males but not in females. The consequent increase in SPNs molecular activity displayed only in male mice indicate that alterations of FSIs in the dorsal striatum are able to produce network and

behavioral changes of potential relevance, acting on SPNs activity state, in a sex dependent manner (*Rapanelli et al., 2017*). This aberrant signaling in SPNs activity after interneuron depletion is not surprising, as local interneurons are a great inhibitory source of SPNs and, among the other striatal interneurons, FSIs exert the majority of GABAergic control of striatal SPNs through feedforward inhibition (*Berke, 2008*). In addition to synapses onto SPNs, striatal FSIs emerged to be synaptically connected with each other through dendritic gap junctions, which potentially allow syncytial activation of groups of FSI establishing a distributed field of inhibition (*Kita et al., 1990*). Taken together, these features suggest a coordinated role in intrastriatal information processing. Upon synchronous activation, FSIs can convert an excitatory input signal, such as salient sensory-related information into a GABAergic inhibitory output signal, shaping in turn SPN activity to downstream basal ganglia nuclei (*Berke, 2008*). Excitatory glutamatergic inputs are conveyed to the striatum mainly from the cortex and thalamus (*Hjorth et al., 2020*). The thalamic Cm/Pf complex (Galvan and Smith, 2011) represents the major source of thalamostriatal connections in primates and non-primates. Cm/Pf-striatal system is not only involved in striatal-mediated physiological functions, such as encoding of action-outcome contingencies (*Bradfield et al., 2013*) but also plays a fundamental role in basal ganglia mediated pathological conditions, such as PD (*Halliday, 2009*) and TS (*Heinsen et al 1996*). However, despite the potential implications for striatal-mediated disorders that emerged to be impacted by sex steroid hormones, the relationship between Cm/Pf-striatal system and gonadal hormones has not been investigated yet. In addition to SPNs, PF afferents contact several types of interneurons (*Smith et al., 2014*), exerting cell-type specificity towards FSIs (*Assous & Tepper, 2019*). Moreover, electrophysiological evidence suggests that PF fibers make stronger excitatory connections onto FSIs than onto striatal principal cells, leading to the idea that excitatory glutamatergic inputs from PF are shaping striatal network activity by strongly influencing FSIs input encoding (*Johansson & Silberberg, 2020*).

Considering the current gaps in understanding, the sexually dimorphic roles of striatal FSIs warrant further investigation. Additionally, the interplay between thalamostriatal connections and sex hormones remains unclear. Our hypothesis posits that the temporal integration of thalamic inputs at the DLS FSIs is sensitive to sex hormones

and the estrous cycle. The underlying mechanism for this sex-dependent modulation of synaptic processing on striatal FSIs may involve changes in FSI cell properties.

During my 3-years research project I have been combining neurophysiological, pharmacological, optogenetic approaches and in-vivo imaging of neuronal population activity (fiber photometry) to develop the following aims:

1- evaluate the presence of differences between sexes, and across estrous cycle phases, in FSIs responsiveness to thalamic glutamatergic input;
2- investigate the effects of sex and estrous cycle in shaping FSI active and passive membrane properties as well as in modulating FSI cell properties, following pharmaceutical alteration of estrogen-mediated signaling;
3- assess the effect of thalamic stimulation onto FSIs during spontaneous locomotor behavior in males and females, and across estrous phases.

Introduction

Sex hormones: from production and release to their impact on brain functions

Sex hormones are a family of hormones comprised of 3 classes: estrogens (also called oestrogens), progestins, and androgens. These steroidal hormones are known to be major regulators of sexual behavior, functions, and physiology, including the reproductive cycle, but they are also emerging as strong regulators of key brain functions, such as memory, cognition, and anxiety-related behavior (*Contrò et al., 2015*).

Synthesis and action mechanism of sex steroid hormones

Production and release of sex steroid hormones are strictly regulated by the hypothalamic-pituitary-gonadal (HPG) axis. Via the release of gonadotrophin-releasing hormone (GnRH), the hypothalamus induces the production of luteinising hormone (LH) and follicle-stimulating hormone (FSH) from the pituitary, stimulating in turn synthesis and release of sex hormones from gonads: ovaries in females and testis in males. Moreover, these sex steroids can directly act on the hypothalamus, regulating GnRH release, and on the pituitary, influencing LH and FSH production (**Figure 2A**). Peripherally sex hormones circulate in the plasma bound to plasma proteins, protecting hormones from metabolic degradation: estrogens and androgens to sex hormone binding globulin (SHBG) while progestins to corticosteroid binding globulin (CBG). A small fraction of free steroid hormones, not bound to any proteins, is also present in plasma and by passive diffusion can readily cross the blood-brain barrier (*Moraga-Amaro et al., 2018*). Those neuroactive steroids (NAS) are steroids that, despite their origin, are capable of modifying neural activities (*Dubrovsky, 2006*).

Moreover, sex hormones' production is not enclosed to the periphery only. The brain itself displays the enzymes needed for the synthesis of these steroids, such as aromatase, significantly contributing to the de novo synthesis of sex hormones. Therefore a significant percentage of sex hormones, among which 17β-estradiol, the most potent estrogen, testosterone, the principal androgen, and progesterone, an essential progestin, can

be found in the brain. Those steroids locally synthesized by the brain are called neurosteroids (NS) (*Dubrovsky, 2006; Moraga-Amaro et al., 2018*).

Sex steroid levels are not stable across mammalian life span. In male humans, the androgen peak occurs at birth and for the first month of life then androgen levels become very low until puberty when they rise to maximum levels and then gradually decline with aging. Estrogen and progestin levels are very low in males (*Plant & Marshall, 2001*). Overall, in adult males, androgen levels are relatively constant with small fluctuations according to the circadian rhythm and the season. In females instead, ovarian hormones, such as estradiol and progesterone levels naturally fluctuate not only across different stages of a female's life but also on a monthly basis. Gonadal hormones are very low prior to puberty in females, after which their levels increase reaching peaks in case of pregnancy and lactation. During post menopause, female hormone levels are very low and except for pathological conditions, androgen levels are generally very low in females. After puberty, estrogen and progesterone synthesis is strictly controlled on a monthly cycle. In humans, this fluctuation of ovarian hormones lasts 28 days and is called the menstrual cycle (*Moraga-Amaro et al., 2018*). During the follicular phase plasma estradiol levels peak, while during the luteal phase, a progesterone peak occurs; between these two phases, ovulation occurs (*Sherman & Korenman, 1975*.) In animal models such as rats and mice, this cycle of estradiol and progesterone is called the estrous cycle and recapitulates humans´ menstrual cycle across a four/five day period. In rodent, a pre-ovulatory increase in estrogen and progesterone levels occurs during proestrus phase. Plasma levels of both ovarian hormones slowly decrease during the following estrus phase although some effects can still be present in tissues, and remain low in the last phase of the estrous cycle, the diestrus (*Proano et al., 2017*) **(Figure 1)**.

These cyclic fluctuations induce large changes in sex steroid concentrations in many tissues, including in the brain (*Morissette et al 1992*), likely affecting several sex-mediated activities controlled by the brain (*Moraga-Amaro et al., 2018*).

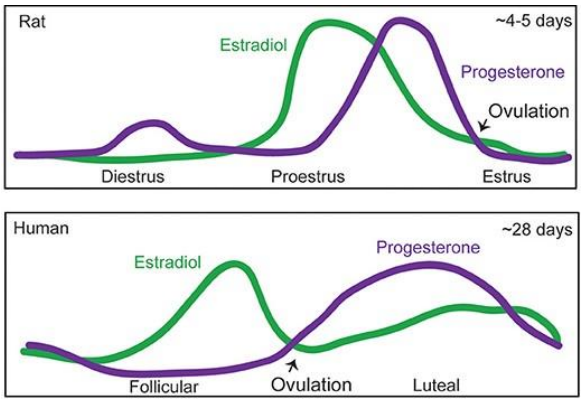

Figure 1. Schematic comparing rodent and human monthly cycle of the two main ovarian hormones, estradiol and progesterone. *Estradiol is indicated in green while progesterone in violet. In rodents, the estrous cycle lasts 4/5 days and it is divided into three phases, diestrus, proestrus, and estrus. Ovulation occurs at the beginning of estrus. In humans, estradiol and progesterone levels change according to a 28 days based menstrual cycle, which can be divided into a follicular and a luteal phase, with ovulation (black arrow) occurring between these phases. Adapted from* (*Moraga-Amaro et al., 2018*).

Sex hormones' action is exerted through their cognate **steroid receptors**, which can be either intracellular, nuclear/cytoplasmic, or membrane-associated. Overall, those receptors belong to the family of hormone-modulated transcription factors and share homology in specific domains of their structure, like the ligand-binding domain (*Vegeto et al., 2007*).

Upon binding to the nuclear/cytoplasmic receptors, the dimerization of the ligand-receptor complex occurs and the assembled dimer migrates to the nucleus; here it activates the specific hormone response elements (HRE) in the promotor region of targeted hormone-responsive genes, either inducing or repressing gene transcription through the recruitment of co-regulators and transcription factors. The effects of this transcriptional-dependent cascade take from 30 minutes to several hours to occur (*Wright et al., 2009*). Specifically in the brain the two intracellular estrogen receptor subtypes, ERα and ERβ, the two progesterone nuclear receptor (nPR) isoforms, PRA and PRB, and the two androgen receptors types ARA and ARB have been identified (*Vegeto et al., 2007*).

Besides this genomic signaling pathway, sex steroid can exert their effects via nongenomic signaling, which is a much more rapid and reversible pathway, and is activated by membrane receptors. Binding their specific G-protein-coupled receptors, such as GPR30 for estrogen, mPR for progesterone, and GPRC6A for androgen, sex hormones induce G protein subunits Gα, Gβ, and Gγ to activate phospholipase C (PLC). Via the second messengers inositol phosphate 3 (IP3+) and diacylglycerol (DAG), PLC can then exert a fast transcription-independent response, which occurs a few seconds to about ten minutes later (*Moraga-Amaro et al., 2018*) **(Figure 2B)**. Interestingly, evidences show that ERα and ERß can be found not only in nuclei and in the cytoplasm but also at the cell membrane, where they induce a number of intracellular events typically induced by activating G-protein coupled receptors. The mechanisms through which ERα and ERβ become associated with the cell membrane is still unclear (*Almey et al., 2004*).

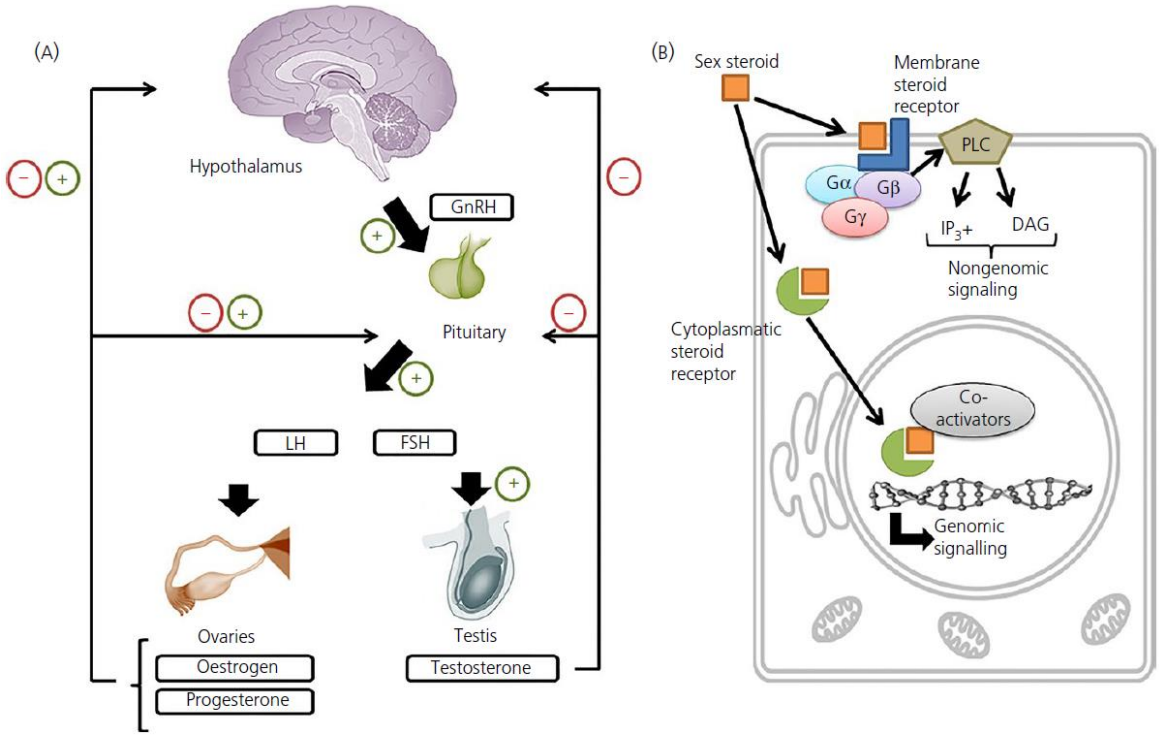

Figure 2. Schematic of sex steroids control at a system level and effects at the cellular level. *(A) Hypothalamic-pituitary-gonadal (HPG) axis regulates the production*

and release of sex steroid hormones. The hypothalamus induces the production of luteinising hormone (LH) and follicle-stimulating hormone (FSH) from the pituitary releasing gonadotrophin-releasing hormone (GnRH). LH and FSH stimulate in turn synthesis and release of sex hormones from ovaries and testis. Sex steroids can directly control this process by acting on the hypothalamus and pituitary. (B) Sex steroids can exert their action through nuclear/cytoplasmic receptors and membrane receptors. Upon binding to the nuclear/cytoplasmic receptors, the dimer composed of ligand-receptor complex migrates to the nucleus where it activates the specific hormone response elements (HRE), either inducing or repressing gene transcription through the recruitment of co-regulators. Binding their specific G-protein-coupled receptors, sex hormones induce the activation of phospholipase C (PLC) by G protein subunits Gα, Gβ, and Gγ. PLC can then exert transcription-independent responses via the second messengers inositol phosphate 3 (IP3+) and diacylglycerol (DAG). Adapted from (*Moraga-Amaro et al., 2018*).

Impact of sex hormones on brain functions

Through genomic or nongenomic signaling pathways sex steroid hormones have been shown **involved in many physiological and pathological conditions** in humans and animal models (*Moraga-Amaro et al., 2018*).

Testosterone emerged to be involved in anxiety-like disorders, as well as in mood disorders and psychosis (*Domonkos et al., 2018*) while estrogens in depression and anxiety (*Kundakovic & Rocks, 2022*). Specifically in humans, women are vulnerable to depression when the levels of sex hormones markedly change concomitantly with the menstrual cycle and during life moments, such as post-partum or menopause. A neuroprotective role for progesterone in seizures, depression, and Alzheimer's disease has instead been shown (*Moraga-Amaro et al., 2018*).

Sex steroids' impact on neural activity also involves the **interaction with neurotransmitter systems**, on which they exert facilitative or inhibitory effects in many brain regions (*Moraga-Amaro et al., 2018*). Among sex hormones, progesterone and estrogen interaction has been more deeply investigated (*Ghomi et al., 2023*). For instance, estrogens have been shown to promote glutamatergic neurotransmission, acting

specifically through NMDA receptors, and to suppress GABA inhibitory inputs while progesterone displays a facilitating effect on GABA neurotransmission through its action at GABAA receptors and an inhibitory influence on excitatory glutamate response (*Moraga-Amaro et al., 2018*). Through these actions, estrogen and progesterone shape synaptic plasticity and subsequently learning and memory in the hippocampus (*Foy et al., 2008*). Furthermore, estrogens have been shown to modulate cognition and mood through interaction with the serotonin (5-HT) system via the regulation of tryptophan hydroxylase enzyme (*Barth et al., 2015*), degradation of 5-HT and the density of 5-HT receptors in brain areas relevant for the control of mood, mental state, and cognition (*Fink et al., 1998*). However, the most studied interaction between estrogen and neurotransmitter systems regards dopamine, as sex hormones emerged able to influence dopaminergic neurotransmission via synthesis, release, turnover, and degradation, pre-and postsynaptic receptors´ density, and transporters affinity (*Barth et al., 2015*). For instance, estradiol levels emerged able to bias decision-making processes, fear extinction, and memory by interaction with dopamine D1-receptor signaling specifically in the dorsal striatum (*Quinlan et al., 2013*).

Although increasing evidence points out an important role of sex hormones in brain-mediated behavior and diseases, the extent to which gonadal and brain-synthetized sex steroids exert their influence still needs to be fully elucidated (*Meitzen et al., 2018*). This investigation is particularly important for brain regions involved in critical behavioral functions, such as motor planning, action selection, motivated behaviors, and cognitive processes, as it is the striatum (*Graybiel & Grafton, 2015*).

Striatum: a key structure in brain functionality sensible to sex hormones

Anatomical description

The striatum is the primary input nucleus to the basal ganglia (*Balleine et al., 2007, Graybiel et al., 1994; Jin and Costa, 2010*). By receiving excitatory glutamatergic inputs, mainly from the cortex and thalamus, the striatum sorts contextual, motor, and reward information and supports the selection of appropriate behaviors through its outputs to downstream basal ganglia structures (*Burke et al., 2017*). Two main efferent pathways rise from the striatum: the direct pathway, which mainly projects to the substantia nigra pars reticulata (SNr), and the indirect pathway, which mostly projects to the external segment of the globus pallidus (GPe). Gpe next targets SNr and the internal segment of the globus pallidus (Gpi), representing together the output nuclei of the basal ganglia (*Báez-Mendoza & Schultz, 2013*) **(Figure 3)**.

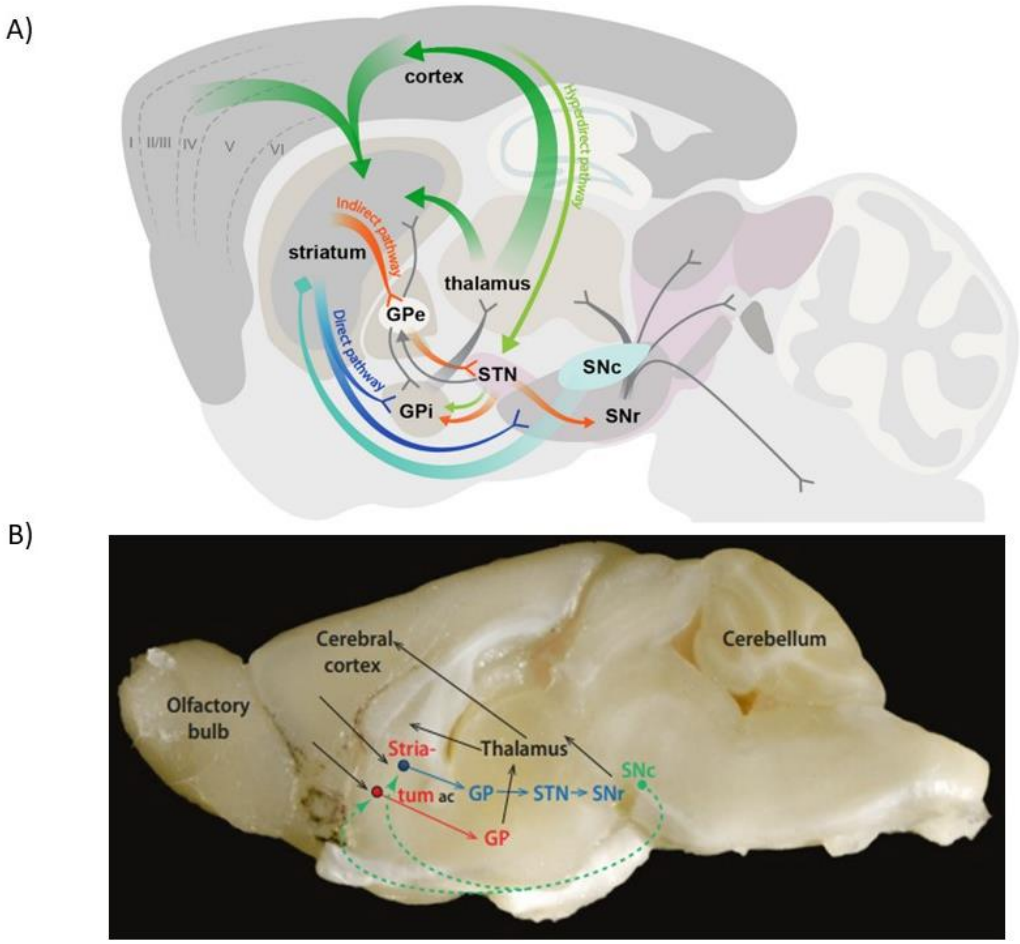

Figure 3. Basal ganglia circuit schematic. (A) *Excitatory glutamatergic input from the cortex and thalamus are integrated into the striatum together with modulatory dopaminergic/cholinergic afferents from substantia nigra pars compacta (SNc) and other brainstem regions. As a result, GABAergic outputs are sent to downstream nuclei thought either direct (shown in blue) or indirect (shown in orange) pathway. Direct pathway efferences target the internal segment of the globus pallidus (Gpi) and substantia nigra pars reticulata (SNr) while indirect pathway sends efferences to the external segment of the globus pallidus (GPe). GPe in turn contacts the subthalamic nucleus (STN), which sends inhibitory projections to Gpi and SNr. Adapted from* (*Blumenstock & Dudanova, 2020*). ***(B)*** *Schematic representation of the main connectivity of the CP/striatum in a midsagittal view of the mouse brain. Here direct pathway is shown in red while the indirect one is indicated in blue. Adapted from* (*Crabtree, 2018*).

The striatum is a heterogeneous structure comprising a ventral portion, which contains the two major divisions of the nucleus accumbens (NAc) and the olfactory tubercle (OT), and a dorsal portion (caudate-putamen or CPu), which are functionally segregated (*Basile et al., 2021*). In general terms, the ventral striatum is known to play a predominant role in reward-related learning and processing motivated behavior (*Báez-Mendoza & Schultz, 2013; Basile et al., 2021; Daniel & Pollmann, 2014*), whereas the dorsal striatum is involved in motor planning, action selection, and stimulus-response habit learning (*Berke, 2008; Graybiel & Grafton, 2015; Zheng et al., 2023*). The ventral striatum comprises also the islands of Calleja complex (ICC), which contains clusters of granule cells and medium-sized and large cells (*Fallon et al.,1983).* In rodents, the ICC is composed of seven distinct clusters within the OT. Although all the functions of the complex still need to be fully elucidated, in rodents it plays a role in reproduction as medium-sized and large cells concentrate substances involved in the reproductive neuroendocrine systems, like luteinizing hormone-releasing hormone and estradiol (*Fallon et al., 1983; Sarret et at., 2017*).

The dorsal striatum in turn can be subdivided into dorsolateral and dorsomedial striatum. **(Figure 4)**. Those two portions are functionally segregated: the dorsolateral striatum is able to formulate stimulus-response strategies such as habit formation and procedural memories that are strengthened during trial-and-error learning, while the dorsomedial striatum is associated with goal-directed learning (*Shu et al., 2019*)

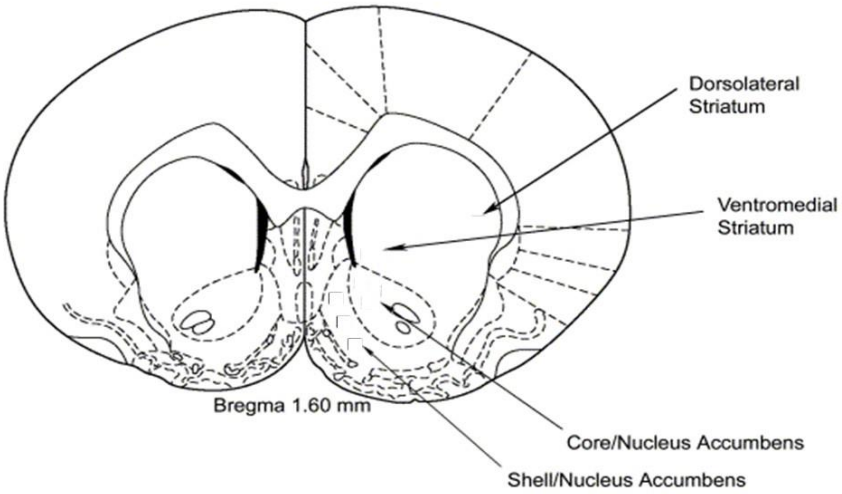

Figure 4. Schematic of dorsal and ventral portions of rat striatum. *Coronal section of the rat brain at Bregma 1.60 mm (Paxinos and Watson, 1998) showing regions of the core and shell of the Nucleus accumbens, and the dorsolateral and ventromedial striatum. Adapted from* (*Berlanga, 2006*).

Different highly debilitating dysfunctional conditions such as neurological and psychiatric diseases including Parkinson's disease, Huntington's disease, autism, schizophrenia, depression, and addiction affect directly or indirectly striatal function, highlighting its crucial role in motor planning and action selection (*Burke et al., 2017*).

Sex hormones influence on striatal-mediated behavior and pathologies

Growing evidence suggests that striatum and striatal-related behaviors and pathologies are **sensitive to biological sex and sex steroid hormone fluctuations** in both animals and humans (*Meitzen et al., 2018*).

In animal models, the relationship between sex and striatal-mediated behaviors has mostly been studied in the context of locomotor and sensorimotor responsiveness (*Meitzen et al., 2018*). In rodents, females are generally more active than males, showing increased running-wheel activity, open-field locomotor activity, exploratory behavior, and sensory responsiveness. This augmented activity emerged to be strictly dependent on sex

hormones, as castration reduced locomotor and sensory responses in females and abolished the sex differences observed (*Studelska & Beatty, 1978*). Interestingly, a specific increase in plasma levels of the sex hormone estrogen emerged implicated (*Meitzen et al., 2018*). In 1986, Becker and colleagues showed that in females not only sensorimotor performances were dependent on hormones estrous cycle variation but also that implants of estradiol in the striatum resulted in a significant improvement in locomotor performances (*Becker et al., 1987*). These early investigations were further confirmed by other studies (*Becker, 2016; Meitzen et al., 2018*), pointing out a facilitating role of estrogen during the integration of sensory and motor information within the striatum (*Becker, 2016*).

Sex differences in drug responsiveness have also been extensively investigated. With respect to psychostimulant administration, female rats show an enhanced rate in acquisition of drug self-administration when tested in an operant conditioning chamber in comparison with male rats. Female rats also tend to escalate drug consumption more rapidly than males. Similarly, in humans, women escalate addiction more rapidly than men, and during abstinence from cocaine, amphetamine, and nicotine, they exhibit greater craving and withdrawal symptoms than men. The specific involvement of ovarian hormones in drug consumption has been tested in ovariectomized female rats, which displayed enhanced motivation for drug administration following estradiol treatment (*Becker, 2016*).

Besides addiction, other striatal-mediated disorders exert sex hormones dependency (*Meitzen et al., 2018*). For instance, differential incidence and phenotype between men and women has been reported in TS and ASD (*Rapanelli et al., 2017*). In PD, sex is the strongest risk factor, as men are more prone to develop PD. Moreover, symptoms´ severity and motor coordination have been associated with monthly changes in gonadal hormones in females, pointing out a strong influence of sex hormones in this striatal-mediated disease (*Meitzen et al., 2018*). These findings generalize to other movement disorders, such as dyskinesia, with worsening of symptoms occurring during low estrogen conditions (*Castrioto et al., 2010*). Changes in anxiety-related behaviors and symptoms also emerged to be sex-biased, occurring more prevalent in women than in men,

and influenced by ovarian hormonal change, controlling the onset and maintenance of clinical anxiety in women (*Nillni et al., 2011*).

Sex differences and estrogen sensitivity in striatal-based non-pathological behavior and relevant disorders point out the relevance of understanding the mechanisms underlying sex hormones' action in the striatum (*Krentzel & Meitzen, 2018*).

Striatal populations: a possible substrate for sex hormones actions

Although striatal-related behaviors and pathologies display clear sex dimorphism, the mechanisms by which sex and gonadal hormones influence striatal neuron physiology remain largely unknown (*Meitzen et al., 2018*).

Principal striatal cells: GABAergic spiny projection neurons (SPNs)

Ninety-five percent of striatal neurons consist of medium-sized **GABAergic spiny projection neurons** (*Tepper and Bolam, 2004*). They form the major inputs and the only outputs of the striatum and are traditionally divided according to their projection targets and dopamine receptor expression (Burke et al., 2017). Dopamine receptors are G protein-coupled receptors grouped into two families based on biochemical, pharmacological and physiological features: D1-class (D1 and D5 subtypes) and D2-class (D2, D3 and D4 subtypes) (*Missale et al., 1998; Rivera et al., 2002*).

Part of the SPN population is represented by direct pathway SPNs (dSPNs). dSPNs express Gs- coupled dopamine D1 receptors, coexpressed with the neuropeptides substance P and dynorphin (*Moratalla et al., 1996b*), and project to the ventral tegmental area (VTA), to the substantia nigra pars reticulata, and to the internal globus pallidus, giving rise to the direct pathway of the basal ganglia. The indirect pathway arises from iSPNs (indirect pathway SPNs), which mainly express Gi-coupled dopamine D2 receptors and send dense projections to the external globus pallidus (GP) and the ventral pallidum (VP) (*Burke et al., 2017*). A subset of SPNs that co-express both D1 and D2 receptors are also present in

the adult striatum; this class of SPNs is morphologically distinct from other SPNs but their function is poorly understood (*Bertran-Gonzalez et al., 2008; Gagnon et al., 2017*).

SPNs display typical intrinsic and firing properties, such as hyperpolarization resting membrane potential close to the potassium equilibrium potential, partly due to inwardly rectifying potassium channels (IKir), and a delayed first action potential in response to depolarizing current step stimulation (*Nisenbaum & Wilson, 1995; Uchimura et al., 1989*). Despite these general characteristics, D1 and D2 expressing SPNs show peculiar electrophysiological characteristics. For instance, D1 SPNs display a lower input resistance, membrane resistance, and membrane time constant in comparison with D2 SPNs together with a greater rheobase (*Gertler et al., 2008*) **(Figure 5)**.

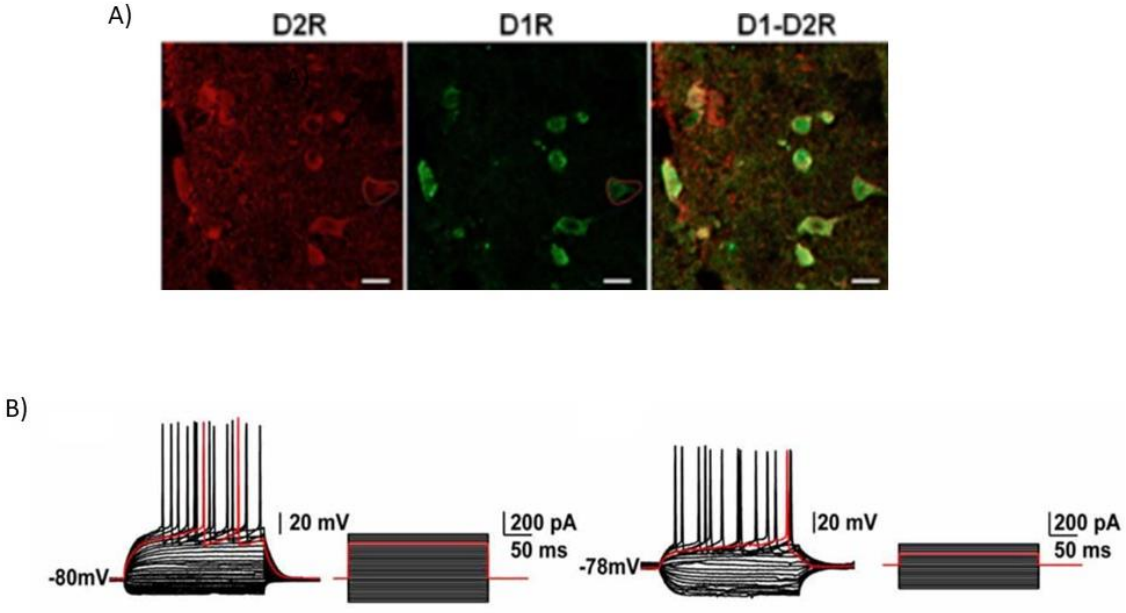

Figure 5. Receptors' expression and neural firing pattern of D1 and D2 expressing SPNs. (A) *Double immunofluorescence staining of D2 (red) and D1 (green) receptors) in dorsolateral striatal brain sections. Scale bar = 10 μm. Adapted from (Kumar and Babu., 2020).* ***(B) Left.*** *Electrophysiological traces obtained in a D1 neuron recorded by patch clamp showing the typical delay-firing pattern in current clamp mode.* ***(Right)*** *Electrophysiological traces obtained in a D2 neuron showing the typical delay firing pattern and a smaller rheobase compared to D1 cells. Rheobase is defined as the first*

current step able to elicit an action potential is highlighted in red. Scale bar = 20 μm. Adapted from (Ren et al., 2017).

SPNs and sex hormones' modulation

In rodents, SPNs do not exhibit sex differences in soma size or neuron density (*Wong et al., 2016*), but they do exhibit dimorphism in functional electrophysiological properties (*Wong et al., 2016*). Experiments performed in whole-cell current clamp configuration on acute brain slices of rat dorsal striatum displayed dissimilarities in SPN active electrophysiological properties between sexes. Females exhibited increased intrinsic excitability compared with male SPNs, as shown by increased evoked action potential in response to excitatory current injection slope, hyperpolarized threshold, and decreased after hyperpolarization magnitude. No sex differences were detected in passive electrophysiological properties. When recorded from gonadectomized males and females, differences in active properties were abolished, proofing that the presence of the estrous cycle was needed to induce sex differences in SPNs (*Dorris et al., 2015*). All recordings were performed in presence of GABAA receptor antagonist picrotoxin (150 μM), NMDA receptor antagonist D-AP5 (10 μM), and the AMPA receptor antagonist DNQX (25 μM). However, the exact electrophysiological and molecular mechanisms driving these changes in dorsal striatum SPN properties remain to be elucidated (*Krentzel & Meitzen, 2018a*).

In the NAc, alterations in active SPNs´ electrophysiological properties came up to be highly sensitive to endogenous hormone fluctuations, as they robustly change across the adult female estrous cycle. Whole-cell current clamp recordings from SPNs in males and cycling females revealed a reduction in intrinsic neuronal excitability in females during proestrus and estrus compared to females in the diestrus phase and males. Conversely, SPNs´ excitatory synaptic input properties, assessed in the same experiment as mEPSC frequency and amplitude, were generally elevated during proestrus and estrus in comparison to diestrus and males (*Proaño et al., 2018*). Across the estrous cycle, proestrus and estrus display the highest estrogen concentration, while during diestrus the plasma levels of estrogen are at a minimum. On the base of the electrophysiological data described, estrogen has been proposed as a critical hormone to facilitate sex differences within the striatum, decreasing SPN intrinsic excitability during peak phases of proestrus and estrus.

The decreased neuronal excitation results in turn in a reduction of GABA release from striatal SPNs and therefore of signaling to downstream basal ganglia structures (*Krentzel & Meitzen, 2018a*).

Collectively those data indicate that sex and natural hormone cycle in females shape striatal SPN electrical properties, including excitatory synapse function (*Krentzel & Meitzen, 2018a*), providing insight into the mechanism that possibly contributes to sex differences in striatal-associated behavior and pathologies (*Proaño et al., 2018*).

Although evidence highlights that gonadal hormones, and estrogen primarily, are important and sex-specific modulators of SPNs´ electrophysiological properties, the exact mechanisms by which they exert their actions have not been fully explained (*Krentzel & Meitzen, 2018a*). One proposed model for estrogen actions on striatal networks involves membrane estrogen receptors (*Krentzel & Meitzen, 2018a*), expressed both on axon terminals, somas, and dendritic spines of striatal SPNs (*Almey et al., 2015; Krentzel et al., 2022*). Nevertheless, a thorough analysis of estrogen receptors´ expression across striatal SPN subtypes, sex, and estral phases has not been performed and nuclear estrogen receptors may be involved too (*Krentzel & Meitzen, 2018a*).

Besides the direct actions on SPNs, estrogen, and other sex hormones may act also on striatal interneurons, which synapse onto SPNs (*Krentzel & Meitzen, 2018a*), thus shaping striatal network activity and leading to differences across sex and estral phases (*Chuhma et al., 2011*). Estrogen receptors have been reported not only on SPNs but also on striatal cholinergic interneurons leading to the idea that sex hormones could modulate striatal functions with substantial variation according to the receptors' expression and location (*Almey et al., 2012*).

Striatal interneurons: an overview

The striatum is not only comprised of SPNs as the remaining 5% of striatal neurons consist of several populations of interneurons that have been classified based on their intrinsic electrophysiological properties, neurochemical and/ or molecular expression profiles. There is only one population of cholinergic interneurons but several diverse and heterogeneous groups of GABAergic interneurons (*Burke et al., 2017*) **(Figure 4)**.

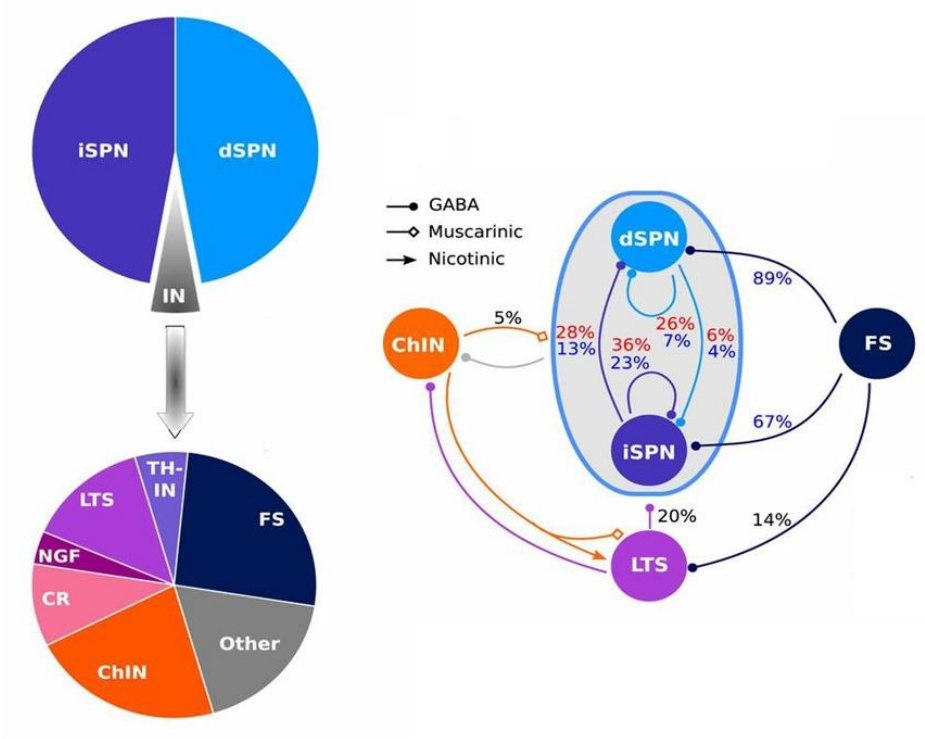

Figure 6. Schematics of striatal neural subtypes and microcircuit organization. ***(Left)*** *The striatal microcircuit is mainly composed of striatal projection neurons (SPNs), classified into two pools of cells, dSPN and iSPN, according to their projection targets. dSPNs give rise to the direct pathway while iSPNs to the indirect pathway. A small percentage (5%) of striatal neurons is composed of interneurons, including parvalbumin-expressing fast-spiking (FS), tyrosine hydroxylase positive interneurons (THINs), low-threshold spiking (LTS) interneurons, neurogliaform (NGF) cells, calretinin-positive cells (CR), and cholinergic interneurons (ChINs).* ***(Right)*** *The schematic shows the connection probabilities within and between striatal neuronal subtypes. Red numbers correspond to connection probability between neurons within 50 μm somatic distance, while blue numbers refer to 100 μm. Adapted from (Hjorth et al., 2020).*

Among striatal interneurons, the most studied include:

ChIN Cholinergic interneurons, also referred to as Tonically Active Neurons (TAN), are large tonically active neurons that release acetylcholine, being the only not GABAergic striatal interneurons (*Zhou et al., 2002*). ChINs give rise to wide axonal arborizations, able to profoundly influence striatal function (*Gonzales and Smith, 2015*).

LTSI Low threshold Interneurons are tonically active GABAergic interneurons. As the name suggests, they exhibit low-threshold Ca2+ spikes and can be identified according to the expression of somatostatin (SOM), nitric oxide synthase (NOS), and neuropeptide Y (NPY) (*Zhou et al., 2002*).

TH In Tyrosine hydroxylase interneurons get their name from their tyrosine hydroxylase (TH) expression. Besides the TH expression, TH interneurons do not express the other enzymes or transporters needed to act as dopaminergic neurons and exert GABAergic inhibition on SPNs (*Xenias et al., 2015*)

NGIF Neurogliaform Interneurons display a complex dendritic arborization and a long-lasting spike afterhyperpolarization, which is their principal characteristic (*Tepper et al., 2018*).

CR Calretinin-expressing interneurons express the calcium-binding protein (CBP) calretinin and are the most abundant type of interneurons in primates' striatum (*Garas et al., 2018*).

FSI Fast-spiking interneurons are the best-studied subtype of the GABAergic interneurons. Striatal FSIs do not exhibit spontaneous activity and frequencies in response to strong depolarizing current injections they can fire at high frequencies (*Berke, 2011*) **(Figure 5)**; their name comes from this hallmark property. Moreover, based on their expression of the Calcium buffering protein parvalbumin (PV), they are also referred to as PV+ (*Tepper et al., 2018*).

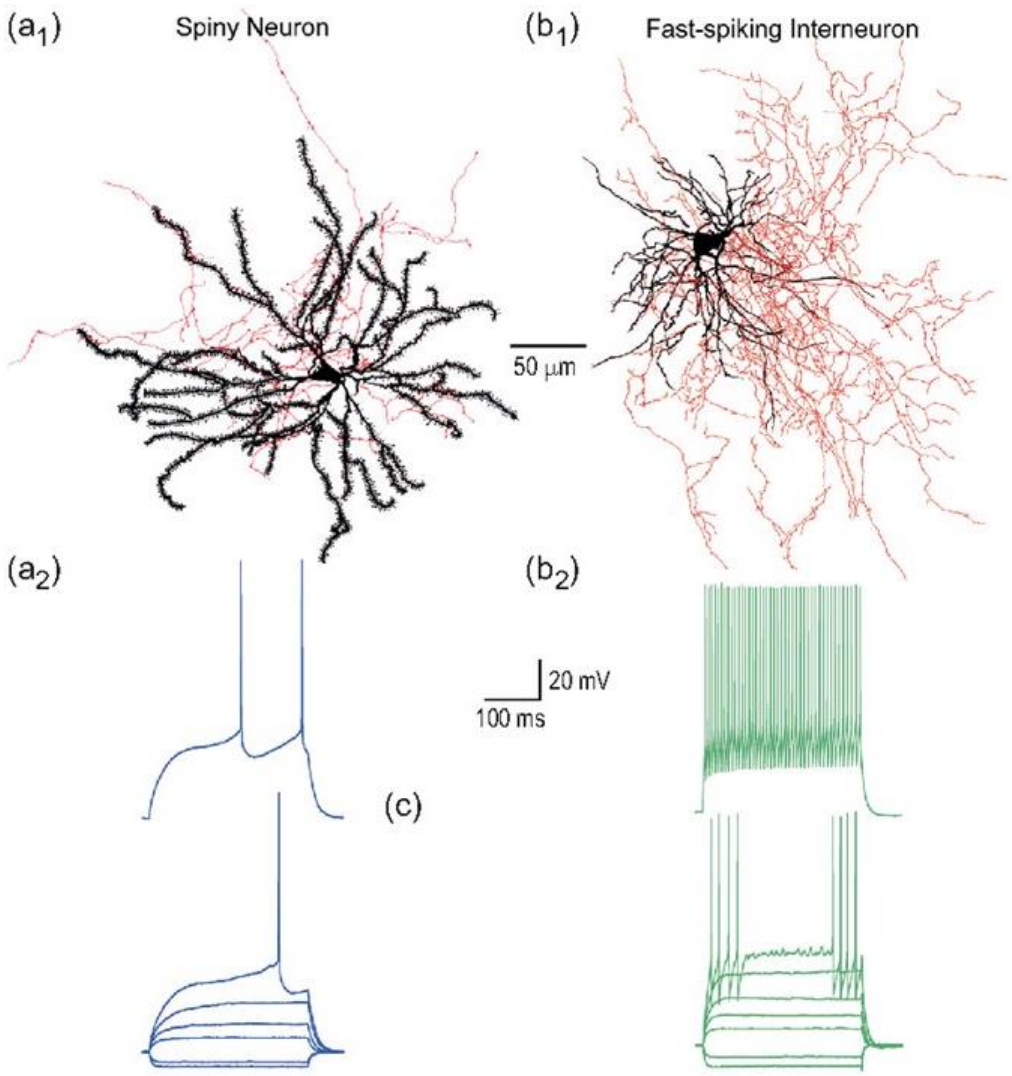

Figure 7. Anatomical and electrophysiological comparison between SPN and FSI. ***(a1)*** *Reconstruction of an SPN obtained from staining with biocytin following intracellular recording in vivo.* ***(a2)*** *In vitro whole-cell current clamp recordings of an adult SPN showing the characteristic marked inward rectification and long latency to first spike following suprathreshold-depolarizing current injections.* ***(b1)*** *Reconstruction of an FSI obtained from staining with biocytin following whole-cell recording in acute brain slice. In comparison with SPN, FSI displays shorter dendrites and an extremely dense local axonal field.* ***(b2)*** *In vitro whole-cell current clamp recordings of FS interneuron showing the characteristic episodic burst firing and the high-frequency firing in response to*

depolarizing current injections. In anatomical reconstructions, soma and dendrites are highlighted in black while axons in red. Adapted from (Tepper et al., 2004).

Striatal interneurons and sex differences: an unexpected role for FSIs

The relationship between striatal interneurons and sex hormones has been investigated only from a behavioral point of view (*Krentzel & Meitzen, 2018*).

In a recent paper from Rapanelli and colleagues (*Rapanelli et al., 2017*), the specific involvement of dorsal striatal CINs and FSI in sex dimorphism was assessed concerning ASD and TS. Both pathologies are sex-biased, being more common in males than females (*Redfield et al., 2014*), and display comorbidity patterns and basal ganglia circuitry implications (*Clarke et al., 2012*). Using a combined transgenic-viral strategy in both male and female mice, single or conjoint depletion of dorsal striatum CINs and/or FSIs was tested. Conjoint depletion of both interneurons or depletion of FSIs only generated ASD and TS-like behavioral abnormalities in males but not in females. When CINs-only ablation was tested, pathological traits such as social behavior impairments, stereotypic behaviors, and anxiety-like behaviors were not observed in both sexes, suggesting a potential relevance of FSIs-specific disruption in sex-dependent striatal behaviors and pathology.

The estrous cycle stage of female mice was not assessed during behavioral experiments, therefore the possibility of a gonadal hormone modulation of the observed effects is still open (*Rapanelli et al., 2017*).

In the same experiment, the downstream effect on activity-dependent signaling in dorsal striatal SPNs was also evaluated. After FSIs depletion, male SPNs displayed increased phosphorylation in molecular markers like rpS6 (*Rapanelli et al., 2017*), a regulator of activity-dependent translation (*Biever et al., 2015*), MSK1 T58 (*Rapanelli et al., 2017*), a marker of the MAPK cascade (*Day & Sweatt, 2012*), and H3 S10 (*Rapanelli et al., 2017*), a marker of epigenetic changes (*Day & Sweatt, 2012*), suggesting a general increase in SPNs activity. These data indicate that specific disruption of FSIs in the dorsal striatum is

sufficient to produce network and behavioral changes of potential relevance, acting on SPNs´ activity state, in a sex-dependent manner (*Rapanelli et al., 2017*).

This aberrant signaling in SPNs activity after interneuron depletion is not surprising, as local interneurons are a great inhibitory source of SPNs and, among the other striatal interneurons, FSIs exert the majority of GABAergic control of striatal SPNs through feedforward inhibition (*Berke, 2008*).

The probability of a synaptic connection between an FSI and an SPN is extremely high, ranging between 48 and 75%, and is significantly greater than the connection probability between pairs of SPNs, which is consistently reported to be between 10 and 20%.

In addition to synapses upon SPNs, striatal FSIs emerged to be synaptically connected with each other, but not with other striatal interneurons. The presence of gap junctions on dendrites allows additional electric connection between FSIs, potentially enabling syncytial activation of groups of FSI and establishing a distributed field of inhibition (*Kita et al., 1990*).

Taken together those features suggest a coordinated role in intrastriatal information processing. Upon synchronous activation, FSIs can convert an excitatory input signal, such as salient sensory-related information from glutamatergic thalamostriatal projections, into a GABAergic inhibitory output signal, shaping in turn SPNs activity to downstream basal ganglia nuclei (*Berke, 2008*) **(Figure 6)**.

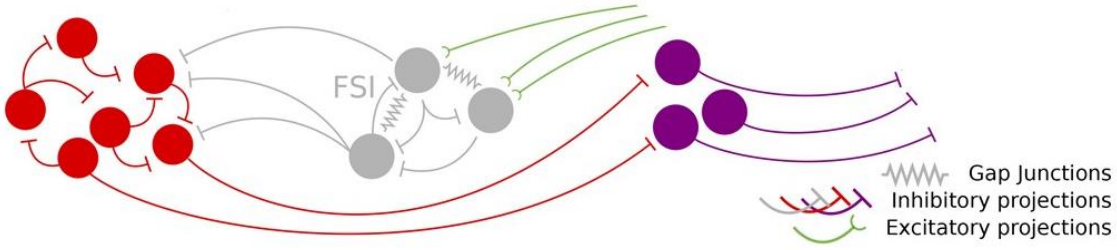

Figure 8. FSIs contribution to intrastriatal information processing. *Being synaptically and electronically connected with each other, FSIs (grey) exert a fine-tuned and*

coordinated feed-forward inhibition on SPNs (red). Upon activation from excitatory projections (green), FSIs strongly influence SPNs inhibitory outputs to other GABArgic structures of basal ganglia (purple), such as GPi (globus pallidus internal segment) or GPe (globus pallidus external segment). Adapted from (Adam et al., 2022).

Understanding how salient extrinsic inputs are processed by striatal circuits, and specifically by FSIs, is essential to understand how these inputs ultimately affect the projection neurons and structures downstream of the striatum (*Berke, 2008*).

Striatal excitatory inputs: focus on the thalamus

The main function attributed to striatum is the selection of appropriate behavior through integration of different inputs conveyed from DRN5-HT neurons (*Steinbusch et al., 1981*) and Substantia Nigra pars compacta (SNc) dopaminergic projections (*Ilango et al., 2014; Rossi et al., 2013*). Dopamine plays a critical role through its interactions with the specific dopamine receptors D1 to D5, which are differently expressed by striatal cell population. For instance, while the D5 receptor subtype is poorly expressed in striatal projection neurons of both the direct and indirect projection pathways, it results highly expressed in interneurons like cholinergic, somatostatin- or parvalbumin-positive neurons. As a consequence of this differential expression in dopamine receptor subtypes, not all striatal neurons are equally responsive to dopaminergic stimulation (*Rivera et al., 2002*).

The pivotal role of striatum in the regulation of motor control, as well as in processing cognitive and emotional inputs, also involved glutamatergic input, mostly conveyed from cortical and thalamic projections (*Hjorth et al., 2020*).While cortex contribution to striatal functionality and behavioral role has been extensively investigated (*Báez-Mendoza & Schultz, 2013b; Daniel & Pollmann, 2014*), the precise role of the thalamostriatal system still needs to be fully elucidated (*Crabtree, 2018; Smith et al., 2014*). Besides the cortex, the thalamus constitutes a major source of excitatory glutamatergic input providing sensory, attentional, and salience information to the striatal network (*Aoki et al., 2015*). Located in the diencephalon, the thalamus is comprised of a large number of nuclei engaged in specialized functions **(Figure 9)**. Exogenous stimulus driven information together with endogenous internally generated information are conveyed in thalamic nuclei from visual, auditory, somatosensory systems and sensorimotor structures. After being

processed in the thalamus, information is converted in outputs to cortical-subcortical

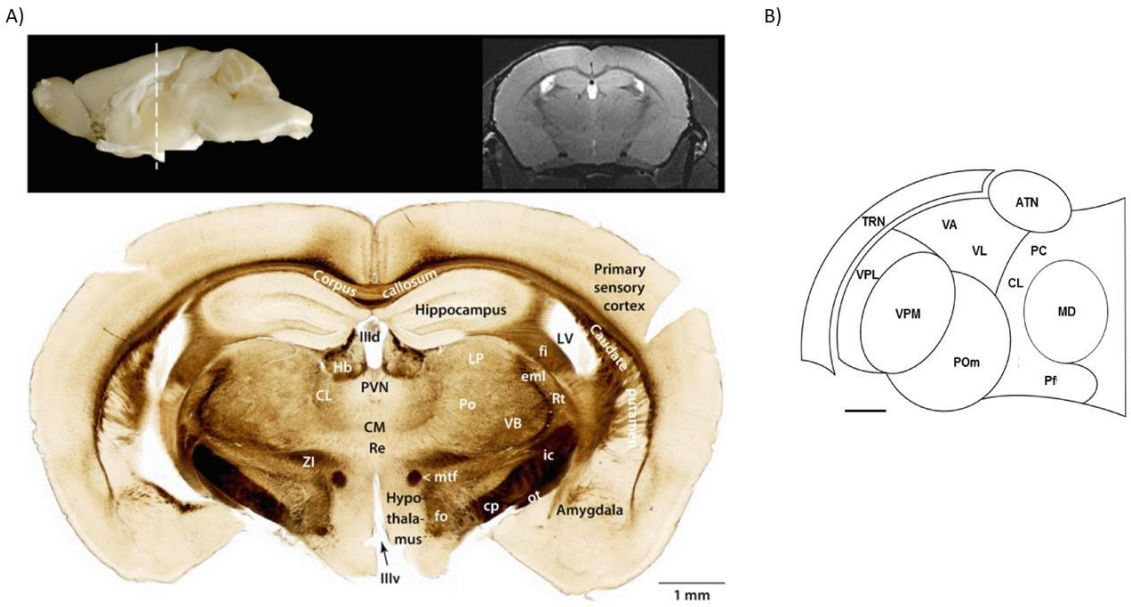

structures, which include basal ganglia and therefore the striatum (*Crabtree, 2018*).

Figure 9. Schematics depicting thalamus position in rodents brain and relative nuclei composition. *(A) Upper part: Location of the thalamus in the mouse brain (indicated by the white line) and relative coronal vibratome section. Lower part: MRT image. Abbreviations: cp = cerebral peduncle, fi = fimbria hippocampi, fo = fornix, ic = internal capsule, mtf = mammillothalamic fasciculus, ot = optic tract, ZI = zona incerta, IIId/IIIv = dorsal and ventral third ventricle (the lack of the IIIv floor is an artifact), LV = lateral ventricle. Adapted from (Schröder at al., 2020). (B) Locations of some thalamic nuclei from a horizontal section of the rat. Abbreviations: ATN, anterior thalamic nuclei; CL, centrolateral nucleus; MD, mediodorsal nucleus; PC, paracentral nucleus; Pfl, lateral part of parafascicular nucleus; Pfm, medial part of parafascicular nucleus; POm, posterior medial nucleus; TRN, thalamic reticular nucleus; VA, ventroanterior nucleus; VL, ventrolateral nucleus; VPL, ventroposterior lateral nucleus; VPM, ventroposterior medial nucleus. Scale = 500 µm. Adapted from* (Crabtree, 2018).

Thalamostriatal fibers originate from several nuclei, among which the higher-order sensory thalamus posteromedial nucleus (POm), the lateral posterior (LP) and lateral dorsal (LD) nuclei, and the centromedian-parafascicular complex (CM/Pf in primates, which

correspond to only Pf nucleus in rodents) (*Smith et al., 2014*). All those nuclei belong to the group of the higher-order sensory thalamic nuclei, but those thalamostriatal fibers drive different types of information according to the originating thalamic nucleus. Receiving inputs from several visual cortical areas the upper superior colliculus, LP and LD nuclei send visual-related information to the striatum while POm conveys somesthetic inputs originating from trigeminal nuclei and multiple sensorimotor cortical areas. Instead, CM/Pf complex receives inputs from the intermediate and deep layers of the superior colliculus and sends multimodal sensory information to the basal ganglia (*Benavidez et al., 2021*).
Pf projections to the subthalamic nucleus (STN) are responsible for movement initiation, as shown in deep brain stimulation treatments for Parkinson's disease (Watson et al., 2021). Moreover, retrograde tracing studies revealed that ipsilateral Pf nucleus of the thalamus targets GP in rodent, providing an additional route for the Pf to influence basal ganglia circuitry besides striatum (Kinkaid et al., 1991). Nevertheless, based on its preferential target, the primate CM/Pf complex can be divided into five major sub-regions: the rostral third of Pf which innervates mainly the NAc; the caudal two thirds of Pf which project to the CPu; the dorsolateral extension of Pf which targets selectively the anterior putamen; the medial two thirds of CM which innervates the post-commissural putamen; and the lateral third of CM which is the source of inputs the primary motor cortex (M1). Through these projections, the CM/Pf complex access to the entire striatal complex, making the CM/Pf-striatal system a functionally organized network with the power to affect broadly basal ganglia functions (*Smith et al., 2004, 2009, 2010; Galvan and Smith, 2011*).

CM/Pf complex (or Pf only in rodents) massively target dorsal and ventral striatum in a topographically organized manner (*Smith et al., 2014*), therefore representing the major source of thalamostriatal connections in primates and non-primates (*Galvan and Smith 2011*).

PF involvement in striatal-mediated physiological and pathological conditions

CM/Pf complex neurons display relatively long, poorly branched dendrites, which are considered ideal for integrating different types of information from a variety of sources (*Deschênes et al., 1995*). In primates, those neurons have been shown to respond to behaviorally salient visual, auditory, and somatosensory stimuli. When not followed by reward, therefore losing salience, responses to stimuli fade quickly, leading to the conclusion that CM/Pf complex neurons respond to external events that are related to attention (*Matsumoto et al., 2001*). This evidence suggests that acting on striatal system, CM/Pf sensory-evoked responses, play a role in attention shifting, behavior switching, and reinforcement processes (*Matsumoto et al., 2001; Bradfield et al., 2013*).

CM/Pf-striatal system is not only involved in striatal-mediated physiological functions, such as encoding of action-outcome contingencies (*Bradfield et al., 2013*) but also displays a fundamental role in basal ganglia-mediated pathological conditions.

For instance, post-mortem studies on PD patients showed a thalamic neuronal degeneration predominantly affecting the CM/Pf complex. Although a significant neuronal loss was also reported in other thalamic nuclei, the greatest percentage (equal to 30/40% of neurons) was displayed by CM/Pf (*Halliday, 2009*) with consequently robust loss of its inputs to the striatum (*Smith et al., 2014*). In Parkinsonian animal models, estimates of the number of glutamatergic synapses formed by cortical and thalamic terminals (marked respectively with vGluT-1 and vGluT-2) in the striatum showed a greater reduction in vGluT-2 positive terminals rather than in vGluT-1 positive terminals. This suggests that the loss of thalamic glutamatergic inputs to the striatum, mainly due to the predominant neuronal loss in CM/Pf complex, overcomes the loss of cortical terminals (*Villalba et al., 2013*) and highlights a key role of CM/Pf-striatal system.

A significant CM/Pf complex neuronal loss has been found also in other striatal-mediated neurodegenerative diseases, such as TS (*Heinsen et al 1996*). Moreover, evidence coming from ablative treatments in TS patients, suggest a central role for this thalamic nuclear complex in controlling the frequency and severity of tics, which are typical traits of TS (*Krauss et al., 2002*). Deep-brain stimulation (DBS) of CM/Pf complex also showed

beneficial effects on some of the psychiatric components of TS, such as anxiety (*Sassi et al., 2011*).

Although PD and TS are CM/Pf-striatal mediated disorders that emerged to be impacted by sex steroid hormones (see "*Sex hormones influence on striatal mediated behavior and pathologies*" section), the relationship between CM/Pf-striatal system and gonadal hormones has not been investigated yet.

PF exerts cell type specificity towards FSIs

CM/Pf complex may mediate its effects on striatal-mediated behavior and pathologies through a complex regulation of striatal microcircuit (*Smith et al., 2014*).
Ultrastructural evidence, indicates the CM/Pf complex preferentially targets proximal dendritic shafts of SPNs while the cerebral cortex preferentially targets more distal dendrites and dendritic spines (*Sadikot and Raymar., 2009*). The synaptic ordering of inputs on dendrites and spines of indicates the corticostriatal and thalamostriatal projection systems encode information in temporally distinct ways, with the thalamostriatal system conveying precisely timed episodic signals, which may modulate corticostriatal activity (*Ding et al., 2008*).
In rodents, while the principal synaptic target of most non-Pf thalamostriatal projections are SPNs, replicating a pattern of synaptic connectivity similar to the corticostriatal system (*Kemp and Powell, 1971*), PF afferents contact also several types of interneurons in addition to SPNs (*Smith et al., 2014*).

PF excitatory inputs are not homogeneous among interneurons as they show cell-type specificity (*Assous & Tepper, 2019*). A recent paper from Johannson and Silberberg showed that optogenetic stimulation of PF terminals evoked EPSP (excitatory postsynaptic potential) in all the FSIs recorded, similar to what obtained in ChINs. Instead, the totality of LTSIs recorded was not responsive to the optogenetic stimulation (*Johansson & Silberberg, 2020*).

Moreover, when comparing EPSP amplitudes among recorded cells, FSI displayed larger responses than adjacent SPNs, while amplitudes in ChINs were significantly smaller

than in principal neurons or FSIs. These data suggest that the same PF fibers make stronger excitatory connections onto FSIs than onto striatal principal cells, leading to the idea that excitatory glutamatergic inputs from PF are shaping striatal network activity by strongly influencing FSIs´ input encoding (*Johansson & Silberberg, 2020*).

Results

FSIs are the only striatal neurons to express the calcium-binding protein parvalbumin (PV) (*Orduz et al., 2013*). To dissect the potential modulation of FSI by sex hormones, we exploited a PV-Cre knock in mouse line in which the expression of Cre recombinase protein is controlled by the PV promoter region (*Orduz et al., 2013*). This mouse line, when transduced in the DLS, enables the Cre-dependent conditional gene expression in putative FSIs of the desired viruses.

To test how sex and cyclical changes in hormone concentrations concomitant with the different phases of the estrous cycle modulate FSIs, we performed experiments both in male and female PV-Cre mice. The female murine estrous cycle is divided into stages, defined by fluctuations in circulating levels of the ovarian steroid hormones. Changes in cell typology within the murine vaginal canal reflect these underlying endocrine events (*McLean et al., 2012*). The estrous stage was established by performing daily cytological assessments of vaginal smears **(Fig.10)** and mice estrous phases were identified based on the ratio of three main cell types present in vaginal smear samples: nucleated epithelial cells, cornified squamous epithelial cells, and leukocytes. During proestrus, a pre-ovulatory increase in circulating 17-β-estradiol levels occurs and vaginal smears are characterized by almost exclusively nucleated epithelial cells. During estrus, 17-β-estradiol levels decline and vaginal smears from proestrus females display almost exclusive cornified squamous epithelial cells. In diestrus, circulating progesterone levels peak, and smears are predominated by leukocytes (*Proano et al., 2018*).

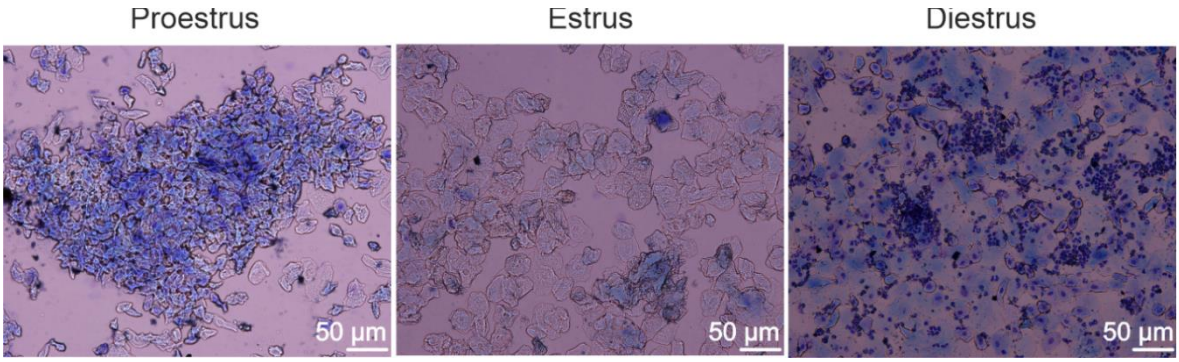

Figure 10. Vaginal estrous cycle stage assay. *Representative images of the three estrous cycle phases sampled by sterile vaginal lavage in female PV-Cre mice. Objective magnification 10X.*

Ex vivo FSI synaptic responsiveness to thalamic glutamatergic input differs in sex and estrous cycle-dependent manner.

The parafascicular nucleus of the intralaminar thalamus (Pf) is known to receive multimodal sensory inputs (*Yamasaki et al., 1986; Nothias et al., 1988; Grunwerg and Krauthamer, 1992; Krout et al., 2001; Coizet et al., 2007; Schulz et al., 2009; Alloway et al., 2014*), which are in turn delivered to downstream structures at different frequencies that may entrain neural activity depending on the estrous cycle phase. Previous works demonstrated a correlation between women auditory responses to the 40Hz stimulation frequency and their levels of the estrogen 17β-estradiol (*Bulanova et al., 2014*).

To investigate the effect of sex and sex-hormone fluctuations on Pf-FSI synapse, we injected a virus bearing the fast channelrhodopsin Chronos (pAAV5-Syn-Chronos-GFP) in the Pf nucleus of PV-Cre mice (K*eppeler et al., 2018*). In the same mice, we also injected a Cre-dependent td-Tomato virus (pAAV9-FLEX-Td-tomato) in DLS (dorsolateral striatum), enabling the Cre-dependent gene expression of the reporter Td-Tomato in putative FSIs (**Fig.11A)**. 4 weeks after injections we verified the expression of Chronos-GFP in DLS-projecting Pf fibers (**Fig.11B**).

On ex-vivo DLS brain slices, we recorded light-evoked excitatory postsynaptic currents (o-EPSCs) of Td-Tomato^{+} FSIs in patch-clamp whole-cell configuration upon optogenetic stimulation of Pf terminals through the microscope objective (10 blue light pulses of 1 ms at 470 nm, 40 Hz) (**Fig.12A**). Putative FSIs were identified by fluorescent visualization of Td-Tomato^{+} (**Fig.12C**) and by their electrophysiological signatures, such as the presence of both single spiking and irregular high-frequency bursts (Berke. 2011). Following optogenetic stimulation, we extracted the charge transfer in response to a train stimulation as a measure of syaptic integration. We measured the charge transfer by integrating the area under the curve of the ten optogenetically evoked EPSCs.

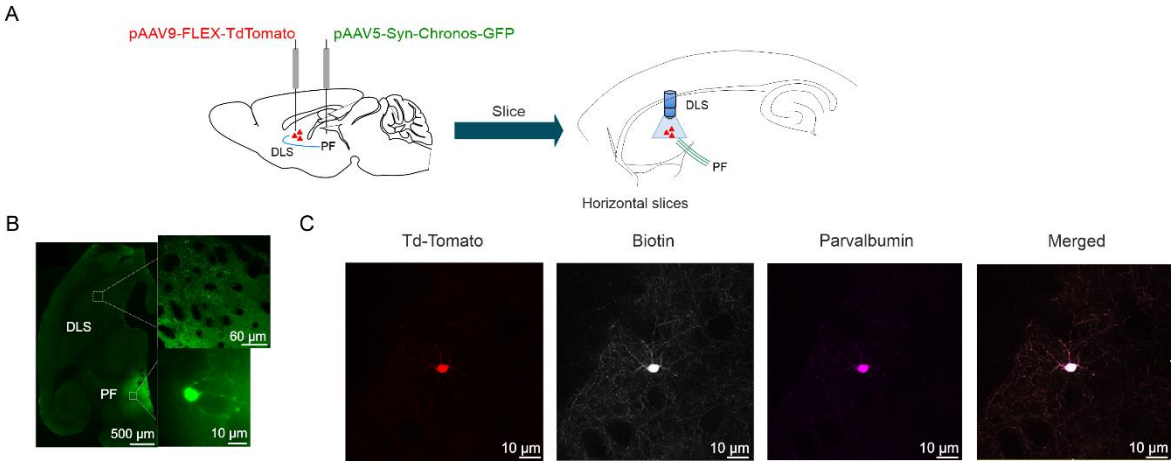

Figure 11. Experimental approach. ***(A)*** *Experimental design. Schematic of FLEX-TdTomato injection in DLS and Chronos-GFP in Pf, and stimulating configuration.* ***(B)*** *Representative image of Chronos-GFP injection site in PF and GFP$^+$ projection fibers in DLS.* ***(C)*** *Representative images of td-Tomato$^+$/Biotin$^+$/Parvalbumin$^+$ recorded cell.*

The analysis of synaptic efficacy measured as charge transfer revealed that FSI responsiveness to Pf train stimulation (40Hz), did not only differ between sexes (*Charge transfer, sex and estrous phases: $F_{3,\ 16}$=21.07; ****p< 0.0001; One way ANOVA)* with males displaying a higher charge transferred compared to all the other cohorts, but also within the estrous phases. That is, FSIs from females in the proestrus showed a reduced charge transfer in comparison to males as well as to females in estrus and diestrus (*Charge transfer, sex and estrous phases: $F_{3,\ 16}$=21.07; ****p< 0.0001; One way ANOVA followed XXX post hoc analysis; male vs proestrus, ****p<0.0001; male vs estrus, **p=0.0044; male vs diestrus, *p=0.0087; proestrus vs estrus, *p= 0.0246; proestrus vs diestrus, **p= 0.005; estrus vs diestrus, p= 0.9471)* (**Fig. 12B-C).**

Overall, our ex-vivo results show that FSI response to excitatory synaptic input varies depending on sex and estrous cycle phases raising the possibility that Pf to DLS-FSI synaptic temporal integration is sensitive to sex hormones. Notably, FSI responsiveness to glutamatergic thalamic stimuli appears to be generally reduced during the proestrus phase and then progressively increased in the following estrous cycle phases, possibly reflecting cycle-related hormonal fluctuations (*Proano et al., 2020*) and cycle-related peaks in estradiol and progesterone plasma levels. These results are consistent with data in literature

indicating that a peak in estradiol levels first followed by a progesterone surge characterizes the proestrus phase. Plasma levels of estradiol and progesterone slowly decrease during the following estrus phase although some effects can still be present in tissues and remain relatively low in the diestrus phase (*Proano et al., 2017, 2023*).

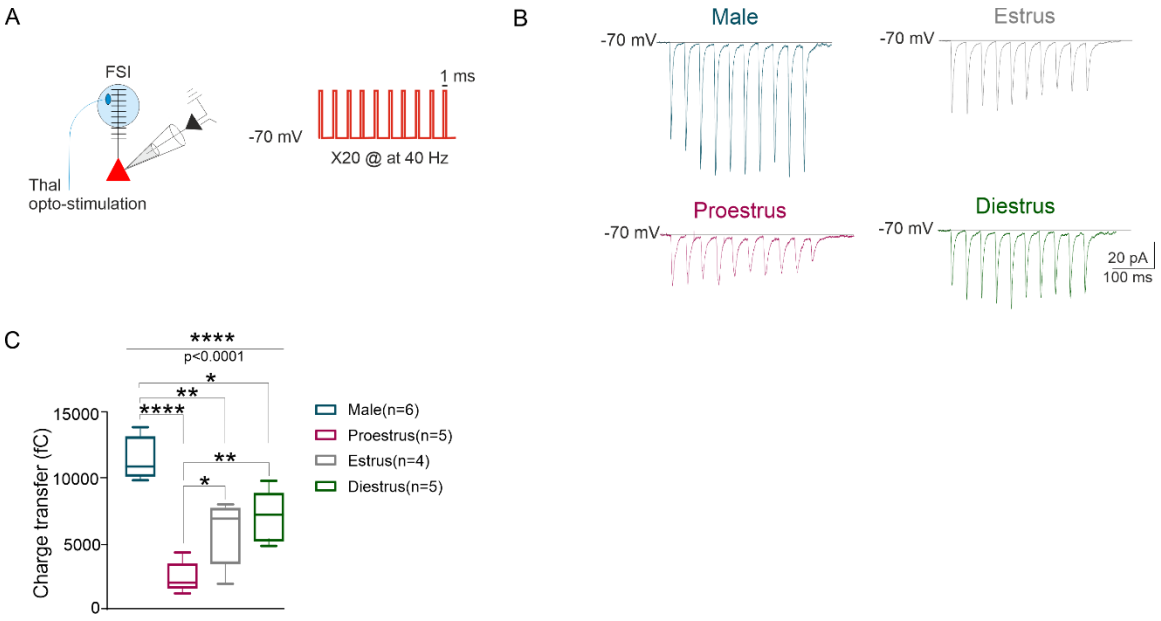

Figure 12. The integration of postsynaptic responses in FSIs to optogenetic stimulation of Pf thalamic inputs, comparing male and female subjects across different estrous phases. ***(A)*** *Schematic of thalamic opto-stimulation protocol.* ***(B)*** *Representative traces of male, proestrus, estrus, and diestrus female FSI responses to optogenetic stimulation in voltage clamp configuration.* ***(C)*** *Box plots summarizing the changes in synaptic strength measured as charge transfer across the different groups {male: cells n=6, mice n=4; 11315± 852.7fC; proestrus: cells n=5, mice n=4; 2403 ± 546.4 fC; estrus: cell n=4, mice n=4; 5858 ± 1060 fC; diestrus: cells n=5, mice n=4; 6990 ± 896.9 fC; Tukey: male vs proestrus, ****p<0.0001; male vs estrus, **p=0.0044; male vs diestrus, *p=0.0087; proestrus vs estrus, *p= 0.0246; proestrus vs diestrus, **p= 0.0052; estrus vs diestrus, p= 0.9471]. The GABAA-receptor blocker GABAzine (10µM) was bath-applied. Box plot extends from the 25th to the 75th percentile, whiskers extend from the minum to the maximum, the bar in the middle of the box shows the median value.*

PPR and AMPA/NMDA ratio at Pf-FSI synapses do not differ between sexes and across estral phases.

So far, our ex-vivo data showed that FSI synaptic responsiveness to optogenetic thalamic stimulation is shaped by sex and by estrous phases (**Fig. 12**). In these experiments, we used a K-methanesulfonate intracellular solution. Although this choice does not allow the achievement of an optimal space clamp, K^+ channels are known to play an important role in filtering synaptic currents at the dendritic level. Thus, using a solution that allows studying all ionic conductances, including K^+ ones, in synaptic integration is crucial for the understanding of this phenomenon. We next investigated ex-vivo the locus of modulation at Pf to DLS-FSI synaptic electrophysiological properties, which are characterized in terms of signal amplitude, kinetics (delay and duration or rise and decay time), and short-term plasticity and depend on the combined properties of the pre- and post-synaptic neurons (*Buzsaki, 1984*).

To this purpose we used a Cesium-gluconate based internal solution, therefore blocking potassium channels to help provide a good space clamp needed to perform connectivity experiments (*Linders et al.,2022*).

Sex hormones are known to exhibit modulatory effects on synaptic transmission. These modulatory effects can be exerted by altering the presynaptic release of neurotransmitters (*Yokomaku et al., 2003*) or the responsiveness or composition of postsynaptic receptors (*Yankova et al., 2001; Maejima et al., 2013*).

We first analyzed the paired-pulse ratio (PPR) of two consecutive stimuli delivered at a short interval to infer changes in presynaptic release probability (*Manabe et al., 1993, Debanne et al., 1996, Dobrunz and Stevens, 1997*). Under the experimental design previously described (**Fig. 11A** *and reported in* **Fig.13A**), on ex vivo brain slices we recorded o-EPSCs of Td-Tomato$^+$ FSIs upon delivery of paired optogenetic stimuli of Pf fibers (40 Hz, 1 ms at 470 nm). We did not observe any significant changes in PPR across groups *(PPR, sex, and estrous phases: $F_{3,17}$=0.449, p = 0.7206; One way ANOVA) (***Fig. 13**). Thus, variations in presynaptic glutamate release probability do not appear to contribute to the observed differences in striatal FSI synaptic responsiveness to thalamic input between sexes and throughout the estrous cycle.

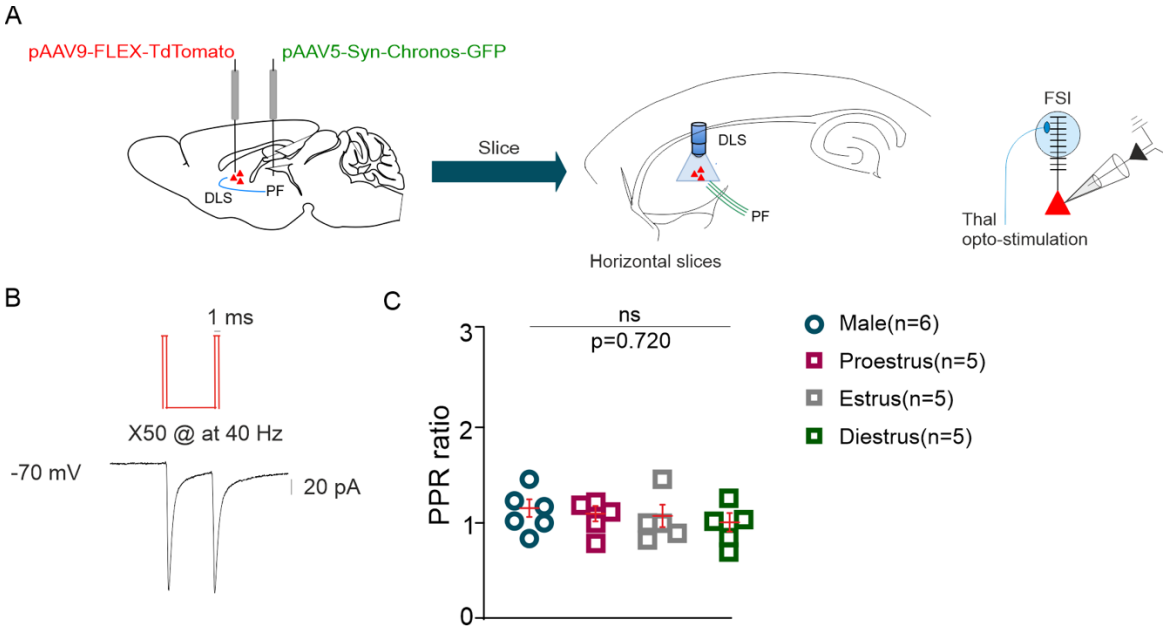

Figure 13. PPR ratio between sexes and across estrous phases. ***(A)*** *Experimental design. Schematic of FLEX-TdTomato injection in DLS and Chronos-GFP in PF, and recording configuration.* ***(B)*** *Schematic of thalamic optogenetic stimulation and representative traces of recorded PPR.* ***(C)*** *Scatter plot summarizing the values of PPR in the different groups. [male: cells=6; mice= 4; 1.087 ± 0.2; proestrus: cells=5; mice= 4; 0.779 ± 0.1; estrus; cells=5; mice= 5; 0.989 ± 0.2; diestrus: cells=5; mice= 4; 1.008 ± 0.2; Tukey: male vs proestrus, p=0.968; male vs estrus, p= 0.911; male vs diestrus, p= 0.668; proestrus vs estrus, p= 0.997; proestrus vs diestrus, p=0.909; estrus vs diestrus, p=0.965]. GABAA-receptor blocker GABAzine (10µM) was bath-applied. Values are expressed as mean ± SEM*

Next, we assessed the postsynaptic strength at Pf-FSI synapses by recording the AMPA/NMDA ratio (**Fig. 11A** *and reported in* **Fig.13A).** We found that the AMPA/NMDA ratio of o-EPSCs was not different across experimental groups *(AMPA/NMDA ratio, sex and estrous phases:* $F_{3,14}$*=0.4103, p = 0.7481; One way ANOVA)* (**Fig. 14**).

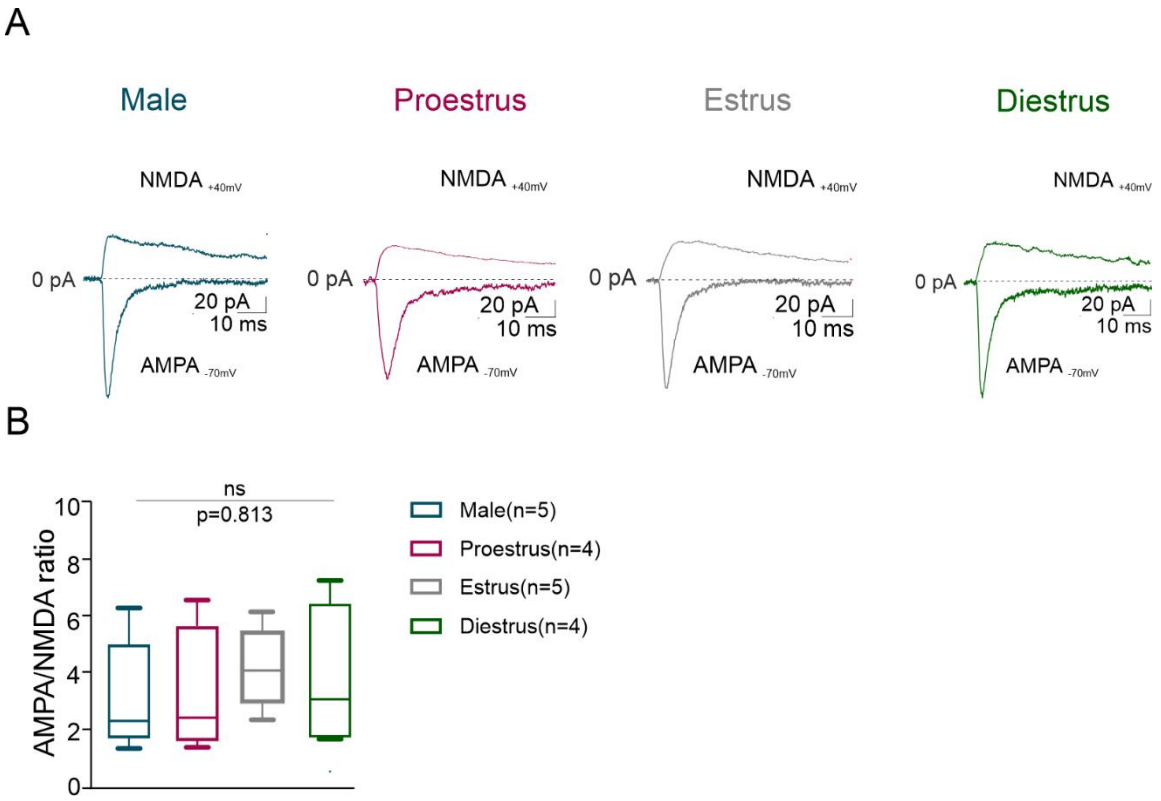

Figure 14. AMPA/NMDA ratio between males and females, and across *estrous* ***phases.*** ***(A)*** *Representative traces of recorded AMPA and NMDA currents in males and females during proestrus, estrus, and diestrus phases.* ***(B)*** *Box plots summarizing the values of AMPA/NMDA ratio in the different groups [male: cells=5; mice= 4; 3.042 ± 0.8; proestrus: cells=4; mice= 4; 3.202 ± 1.147; estrus: cells=5; mice= 3; 4.194 ± 0.6; diestrus: cells=4; mice= 4; 3.755 ± 1.2; Tukey: male vs proestrus, p=0.999; male vs estrus, p= 0.812; male vs diestrus, p= 0.953; proestrus vs estrus, p= 0.887; proestrus vs diestrus, p=0.980; estrus vs diestrus, p=0.988; AMPA amplitude, male = 149.5 ± 93.26 pA; proestrus = 260.1 ± 113.9 pA; estrus = 240.6 ± 116.4; diestrus = 66.89 ± 17.51 pA; NMDA amplitude, male = 52.10 ± 24.68 pA; proestrus = 120.0 ± 36.47 pA; estrus = 97.55 ± 33.82 pA; diestrus = 30.98 ± 13.41 pA]. GABAA-receptor blocker GABAzine (10µM) was bath-applied. Box plot extends from the 25th to the 75th percentile, whiskers extend from the minum to the maximum, the line in the middle of the box shows the median value.*

Collectively, our data indicate that the mechanism underpinning different striatal FSI synaptic integration of Pf input across sexes and estrous phases may be independent of presynaptic release probability and post-synaptic receptor composition or function.

Sex and estrous phases shape FSIs active but not passive properties.

It has been previously shown that sex hormones alter SPN excitability of the ventral striatum (Proano et al., 2017). Since neuron excitability depends on active properties (ion channel activity/distribution) and passive properties, variations in these properties can affect influence how readily a neuron integrate post synaptic depolarization and ultimately it fires in response to incoming stimuli.

To test whether sex and estrous phases modulate synaptic integration of Pf to FSI inputs by regulating changes in FSI excitability, we performed whole-cell patch clamp experiments in TdTomato^{+} cells following AAV9-FLEX-TdTomato injection in DLS (**Fig. 15A**). Ionotropic fast synaptic transmission was blocked by bath-application of GABAA-receptor blocker GABAzine (10µM), NMDA receptor antagonist APV (30µM) and AMPA receptor antagonist NBQX (20µM).

We first tested whether passive membrane FSI electrophysiological properties differed between sexes and across estrous cycle phases. The passive properties of a neuron refer to those properties that do not involve voltage-dependent or synaptically-activated ion channels. These properties determine how a neuron responds to synaptic inputs and contribute to the shaping of both the amplitude and time course of postsynaptic potentials. We therefore measured FSI membrane resistance (Rm), membrane capacitance (Cm), and time constant of the membrane (Tau) in response to a single depolarizing step in voltage-clamp configuration (**Fig. 15B**). No significant changes were detected in Rm, Cm and tau between sexes and across estrous phases (*Rm, sex and estrous phases: $F_{3,47}=0.9232$; $p=0.1404$; One way ANOVA; Cm, sex and estrous phases: $F_{3,47}=0.6941$; $p=0.4276$; One way ANOVA; Tau, sex and phases: $F_{3,46}=0.3389$; $p=0.7498$; One way ANOVA)* (**Fig. 15C**).

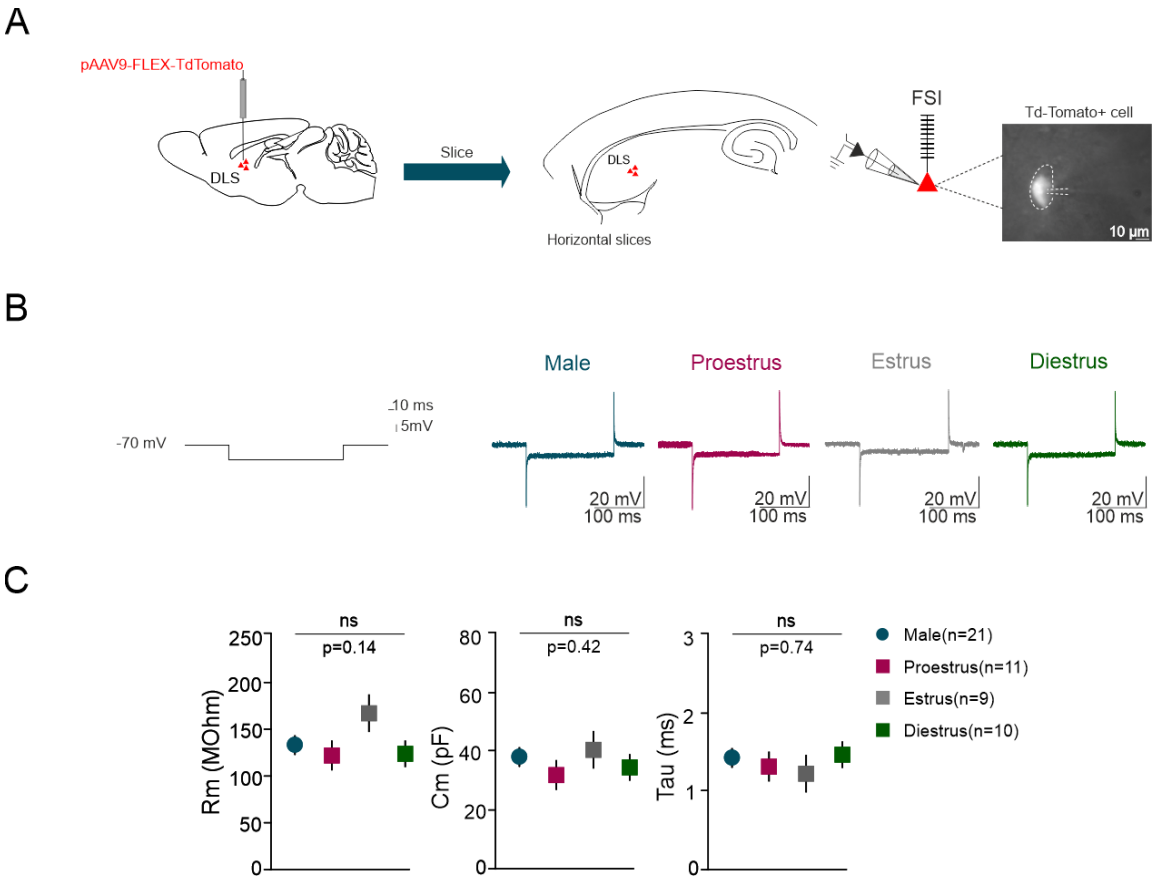

Figure 15. Passive properties between males and females across *estrous* ***phases. (A)*** *Schematic of FLEX-TdTomato injection in DLS, and recording configuration.* ***(B)*** *Representative traces of male, proestrus, estrus, and diestrus female FSI responses to a -5 mV step in voltage clamp configuration.* ***(C)*** *Box plots summarizing average values of membrane resistance (Rm), membrane capacitance (Cm), and tau for each experimental group. [Rm: male: cells=21; mice= 10; 135.1 ± 8.08 MOhm; proestrus: cells=11; mice= 7; 122.9 ± 16.11 MOhm; estrus: cells=9; mice= 6; 168.5 ± 20.25 MOhm; diestrus: cells=9; mice= 8; 124.7 ± 14.37 MOhm; Tukey: male vs proestrus, p=0.8980; male vs estrus, p=0.2930; male vs diestrus, p= 0.9400; proestrus vs estrus, p= 0.1498; proestrus vs diestrus, p=0.9997; estrus vs diestrus, p= 0.1930] [Cm: male: cells=21, 37.85 ± 2.98 pF; proestrus:cells=11; 31.73 ± 2.8 pF; estrus: cells=9; 40.86 ± 6.12 pF; diestrus: cells=10; 34.45 ± 3.34pF; Tukey: male vs proestrus, p= 0.6082; male vs estrus, p= 0.9412; male vs diestrus, p= 0.9096; proestrus vs estrus, p= 0.4305; proestrus vs diestrus, p= 0.9659; estrus vs diestrus, p= 0.7220] [Tau: male: n=21; 1.44 ± 0.12 ms; proestrus: n=11; 1.32 ± 0.18 ms; estrus:*

n=9; 1.24 ± 0.18 ms; diestrus: n=10;1.46 ± 0.12 ms. Tukey: male vs proestrus, p= 0.9328; male vs estrus, p= 0.7784; male vs diestrus, p >0.9999; proestrus vs estrus, p= 0.9880; proestrus vs diestrus, p= 0.9433; estrus vs diestrus, p= 0.8203]. Values are expressed as mean ± SEM

We then assessed the active properties of striatal FSIs by analyzing the initiation and number of evoked action potentials in response to a series of positive current injections (**Fig. 16**). The active electrical properties of a neuron refer to those properties that involved the activation of voltage, ligand, or second messenger gated transmembrane ionic channels, which lead to the generation of action potentials *(Llinas, 2008*).

The rehobase, defined as the first current step capable of eliciting at least one action potential, significantly differed between males and females, and across different estrous cycle phases *(sex and estrous phases: $F_{3,47}$=0.5511, ** p=0.0021; One way ANOVA)*. Rheobase was significantly increased in proestrus-phase females compared with all the other groups (**Fig. 16B**). These results indicate that more depolarizing current is required for initial action potential generation, suggesting that FSIs in proestrus have decreased excitability. This increase in rheobase may be a consequence of the estradiol and/or progesterone peaks occurring during the proestrus phase. Accordingly, no differences were detected in rheboase currents comparing estrus and diestrus phases as these two phases are characterized by lower levels of estrogen and progesterone. We also found that the input-output relationship of striatal FSIs, expressed as the number of action potentials evoked by increasing steps of depolarizing current, differed between males and females in the proestrus phase. (*Input current*: $F_{3,46}$=82.29, p<0.0001; S*ex and estrous phase: $F_{3,46}$=8.47, p=0.0001; Input current X sex and estrous phases: $F_{3,46}$ = 4.843, DF= 24, ****p<0.0001; RM- Two-way ANOVA)* (**Fig. 16C**).

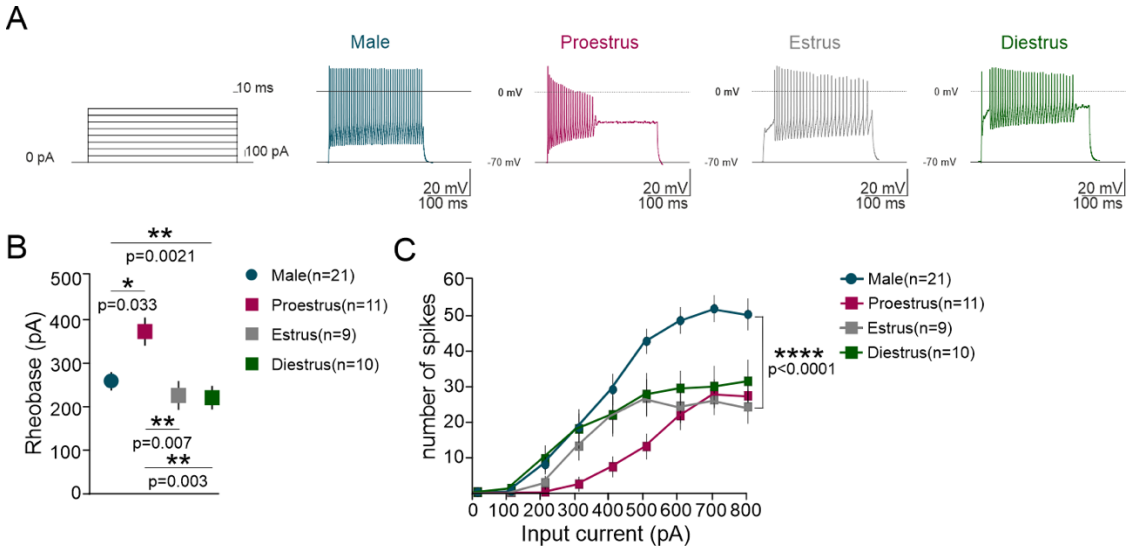

Figure 16. Neuron active properties between males and females across estrous phases. ***(A)*** *Representative traces of voltage responses of male, proestrus, estrus, and diestrus female FSIs to a step of depolarizing current injections of 300 pA.* ***(B)*** *Box plots summarizing average values of rheobase for each experimental group. [male: cells=21; mice= 10; 266.2 ± 19.81 pA; proestrus: cells=11; mice= 7; 365.5 ± 31.89 pA; estrus: cells=9; mice= 6; 221.1 ± 32.42 pA; diestrus: cells=10; mice= 8; 216.0 ± 25.59 pA; Tukey: male vs proestrus, *p=0.0330; male vs estrus , p= 0.6283; male vs diestrus, p= 0.5128; proestrus vs estrus,** p= 0.0070; proestrus vs diestrus, **p=0.0037; estrus vs diestrus , p=0.9994]* ***(C)*** *Time course of the number of action potential evoked by a series of depolarizing current injections*

Pairwise comparison of the input-output relationship of FSIs across estrous phases (**Fig. 17** indicates significant differences between proestrus and estrus (I*nput current: $F_{8,144}$=27.27, p<0.0001; Estrous phase: $F_{1,18}$=3.210, p=0.0900; Input current X proestrus vs estrus: $F_{8,144}$ =2.515, p=0.0137; RM- Two-way ANOVA)* (**Fig. 17A)** and diestrus females *(Input current: $F_{8,152}$=26.60, p<0.0001; Estrous phase: $F_{1,19}$=4.981, p=0.0379; Input current X estrous phase: $F_{8,152}$ =1.886, p=0.0660; RM- Two-way ANOVA)* (**Fig. 17B**), but no differences between estrus and diestrus *(Input current: $F_{8,136}$=20.96, p<0.0001; estrous phase: $F_{1,17}$=0.7400, p=0.4016; Input current X* estrous phase*: $F_{8,136}$ =0.2999, p=0.9649; RM- Two-way ANOVA)* (**Fig.17C**). Thus, intrinsic excitability appears to be generally reduced during the proestrus phase and then progressively increased in the following estrous cycle phases, possibly reflecting cycle-related hormonal fluctuations *(Proano et al., 2020).*

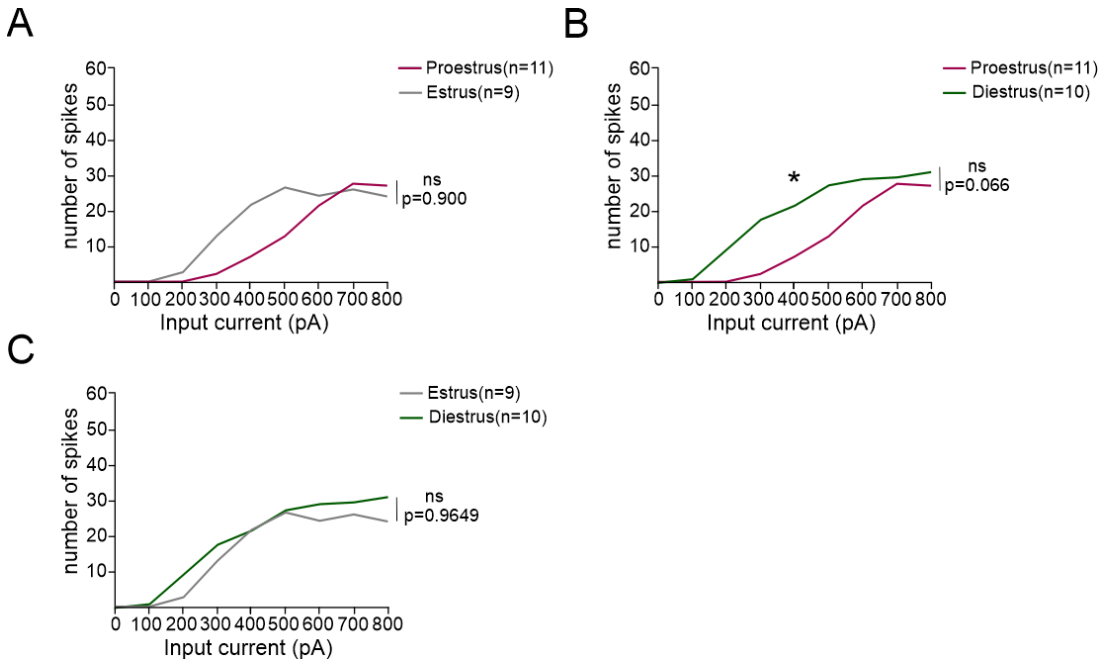

Figure 17. Number of spikes evoked by depolarizing current across estrous phases. (A) *Comparison between proestrus and estrus* ***(B) C****omparison between proestrus and diestrus.* ***(C)*** *Comparison between estrus and diestrus. Values are expressed as means (solid lines from Fig7).*

Pharmacological manipulation of estrogen-mediated signaling exacerbates differences in FSI excitability in proestrus and diestrus phase

So far, our results indicate that sex and estrous phases are characterized by different FSI synaptic responsiveness to Pf thalamic input and FSI excitability. These differences could be due to several factors, including hormonal fluctuations (i.e., fluctuations in estrogen and progesterone concentrations) that can affect synaptic and neuronal properties by directly regulating ion channel and synaptic processes through either genomic and non-genomic actions (*O'Lone et al., 2004., Arand and Pascual, 2001*), and/or by influencing neuromodulatory systems, which in turn can significantly impact synaptic integration and neuronal excitability (*Bourque et al., 2011 McEwen, 2002; Bethea and Reddy, 2012;* see also *"Project implementation"*).

As a first step to elucidate the specific mechanisms behind our results, we tested the hypothesis that in female mice during proestrus, when the circulating levels of estrogen are higher compared to the other estrous phases (*Lovick and Zangrossi, 2021; Krentzel and*

Meitzen, 2018), the activation of membrane-associated estrogen receptors (G-protein coupled estrogen receptor - GPER estrogen receptor, and alpha – ERα - and beta -ERβ- membrane-associated isoforms) modulates FSI excitability, through a non-genomic action (*O'Lone et al., 2004., Arand and Pascual, 2001).* If this is the case, we expect pharmacological manipulation of ER-mediated membrane signaling to rescue excitability differences.

In clinics, a widely used antiestrogen is the compound Fulvestrant, an analogous of 17-β estradiol, which has been primarily designed to destabilize the structure and function of ERα and ERβ in their classical nuclear form (*McDonnell & Wardell, 2010*). Being an analogous of 17-β estradiol, Fulvestrant can also act as a full agonist on GPER (*Fitts et al., 2011*). Notably, adult striatal neurons exclusively express membrane-associated ERα and ERβ, but not nuclear ERs (*Krentzel et al., 2022*). Because of its translational potential, we investigated the effect of acute Fulvestrant application on striatal brain slices.

We assessed passive membrane FSI electrophysiological properties in response to a single depolarizing step in voltage-clamp configuration (*electrophysiological protocol is described in* **Fig. 15A**) following Fulvestrant application (*electrophysiological and pharmacological regime is reported in* ***Fig. 18A****).* Fulvestrant did not elicit any significant difference in Rm, Cm, and tau in FSI recorded in proestrus, estrus, and diestrus (**Fig. 18**) *(Rm: estrous cycle phases: $F_{2, 13}$=0.4737, p=0.6330; Fulvestrant: $F_{1, 13}$=0.002198, p=0.9633; Tukey; estrous cycle phases X Fulvestrant: $F_{2,13}$=0.4663, p=0.6374; RM- Two-way ANOVA) (Cm: estrous cycle phases: $F_{2, 13}$=0.3781, p=0.6924; Fulvestrant: $F_{1, 13}$=0.2936, p=0.5971; estrous cycle phases X Fulvestrant: $F_{2,13}$=0.6021,p=0.5623; RM- Two-way ANOVA) (Tau: estrous cycle phases: $F_{2, 13}$=0.3653, p=0.7009; Fulvestrant: $F_{1, 13}$=0.6664, p=0.4290; estrous cycle phases X Fulvestrant: $F_{2,13}$=0.3327, p=0.7229; RM- Two-way ANOVA).*

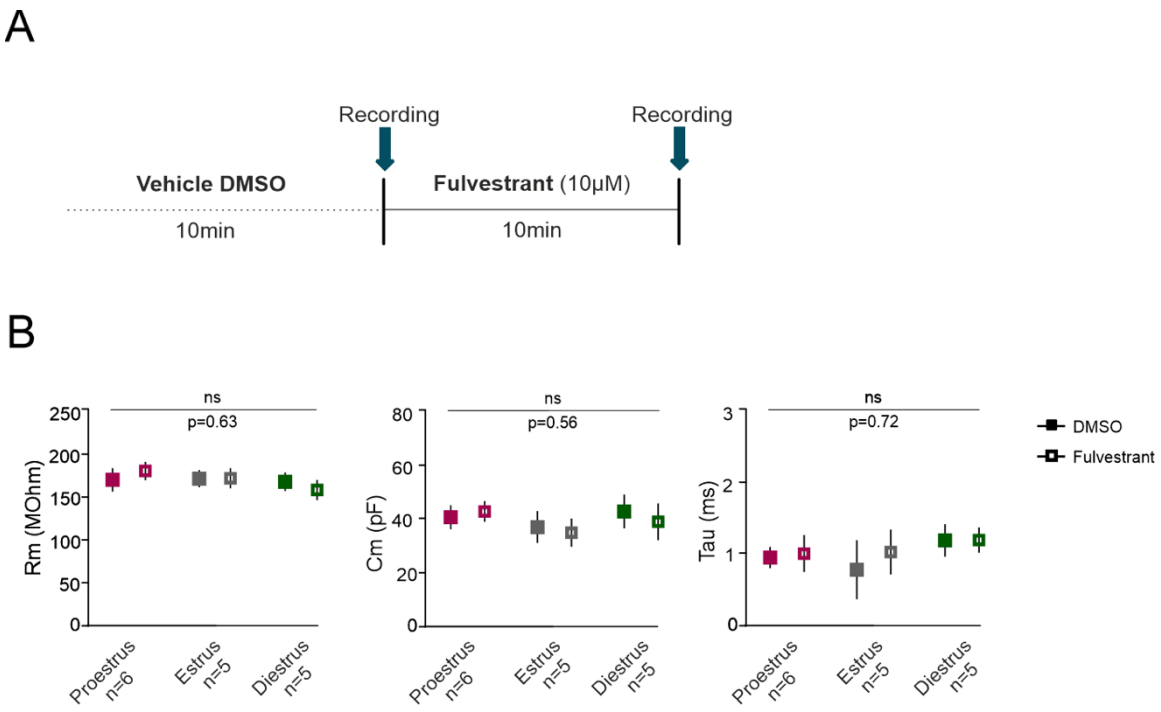

Figure 18. Estrogen agonist effect on passive properties across *estrous* ***phases. (A)*** Schematics illustrating the electrophysiological and pharmacological regime: ex-vivo brain slices were pre-exposed with a vehicle [Vehicle: 0.01% DMSO)]; recordings were then performed on FSI in the presence of vehicle only or Fulvestrant (10µM). (B) Box plots summarizing the average values of membrane resistance (Rm), membrane capacitance (Cm), and tau during the vehicle (minutes 9-10) and after bath application of Fulvestrant (minutes 9-10) [Rm: proestrus:cells=6; mice=4; DMSO168.0 ± 13.40 MOhm vs Fulvestrant 178.1 ± 10.57 MOhm; p= 0.8513; Sidak; Estrus: cells=5; mice= 4; DMSO 169.3 ± 9.817 MOhm vs Fulvestrant 169.7 ± 11.56 MOhm; p>0.9999; Sidak; Diestrus: cells=5; mice= 4; DMSO 165.8 ± 10.75 MOhm vs Fulvestrant 156.4 ± 11.66 MOhm; p= 0.9037; Sidak] [Cm: proestrus: cells=6; mice= 4; DMSO 41.19 ± 3.364 pF vs Fulvestrant 42.77 ± 2.898 pF;p= 0.9292; Sidak; Estrus: cells= 5; mice= 4; DMSO 38.45 ± 4.437 pF vs Fulvestrant 136.89 ± 3.930 pF; p= 0.9471; Sidak; Diestrus: cells=5; mice= 4; DMSO 42.77 ± 4.687 pF vs Fulvestrant 39.91 ± 5.123 pF; p= 0.7549; Sidak] [Tau: Proestrus: cells= 6; mice= 4; DMSO 0.8865 ± 0.0988 ms vs Fulvestrant 0.9229 ± 0.1709 ms ;p= 0.9912; Sidak; Estrus: cells=5; mice= 4; DMSO 0.7730 ± 0.2740 ms vs Fulvestrant 0.9381 ± 0.2082 ms; p= 0.6394; Sidal; Diestrus: cells=5; mice= 4; DMSO 1.045 ± 0.1511 ms vs Fulvestrant 1.049 ± 0.1174 ms; p>0.9999; Sidak]. Values are expressed as mean ± SEM.

We next analyzed Fulvestrant effects on FSIs action potential initiation and generation in response to a series of positive current injections (**Fig.19**) (*electrophysiological protocol is described in* **Fig. 16A**). Surprisingly, in proestrus-phase females, Fulvestrant strongly reduced the number of spikes evoked by current steps *(Proestrus: Input current: $F_{8,40}$=13.89, p<0.0001; Fulvestrant treatment: $F_{1,5}$=10.55; p=0.0227; Input current X Fulvestrant treatment, $F_{8,40=}$ 5.476,, ****p=0.0001; ;RM- Two-way ANOVA) (***Fig.19A**). Accordingly, action potential initiation, measured by the rheobase, strongly increased following Fulvestrant application (*Proestrus: DMSO vs Fulvestrant treatment, *p=0.0408; Sidak)* (**Fig.19D**). In estrus instead, we did not find any significant differences in the number of spikes evoked *(Estrus: Input current: $F_{8,32}$=6.612,, p<0.0001; Fulvestrant treatment: $F_{1,4}$=0.1121; p=0.7545; Input current X Fulvestrant treatment, $F_{8,32=}$ 0.2982,, p=0.9613;; RM- Two-way ANOVA)* (**Fig. 19B)** nor in the rheobase (*Estrus: DMSO vs treatment, p=0.9956; Sidak)* (**Fig. 19D).** Also in diestrus, Fulvestrant exerts significant effects on FSIs´ input-output function *(Diestrus: Input current: $F_{8,32}$=11.92, p<0.0001; Fulvestrant treatment: $F_{1,4}$=0.1825; p=06912; Input current X Fulvestrant treatment, $F_{8,32=}$ 3.670, **p=0.0039; RM- Two-way ANOVA)* (**Fig. 19C**) and on rheobase, which resulted significantly increased after agonist application (*Diestrus: DMSO vs Fulvestrant treatment, **p=0.0013; Sidak)* (**Fig. 19D).**

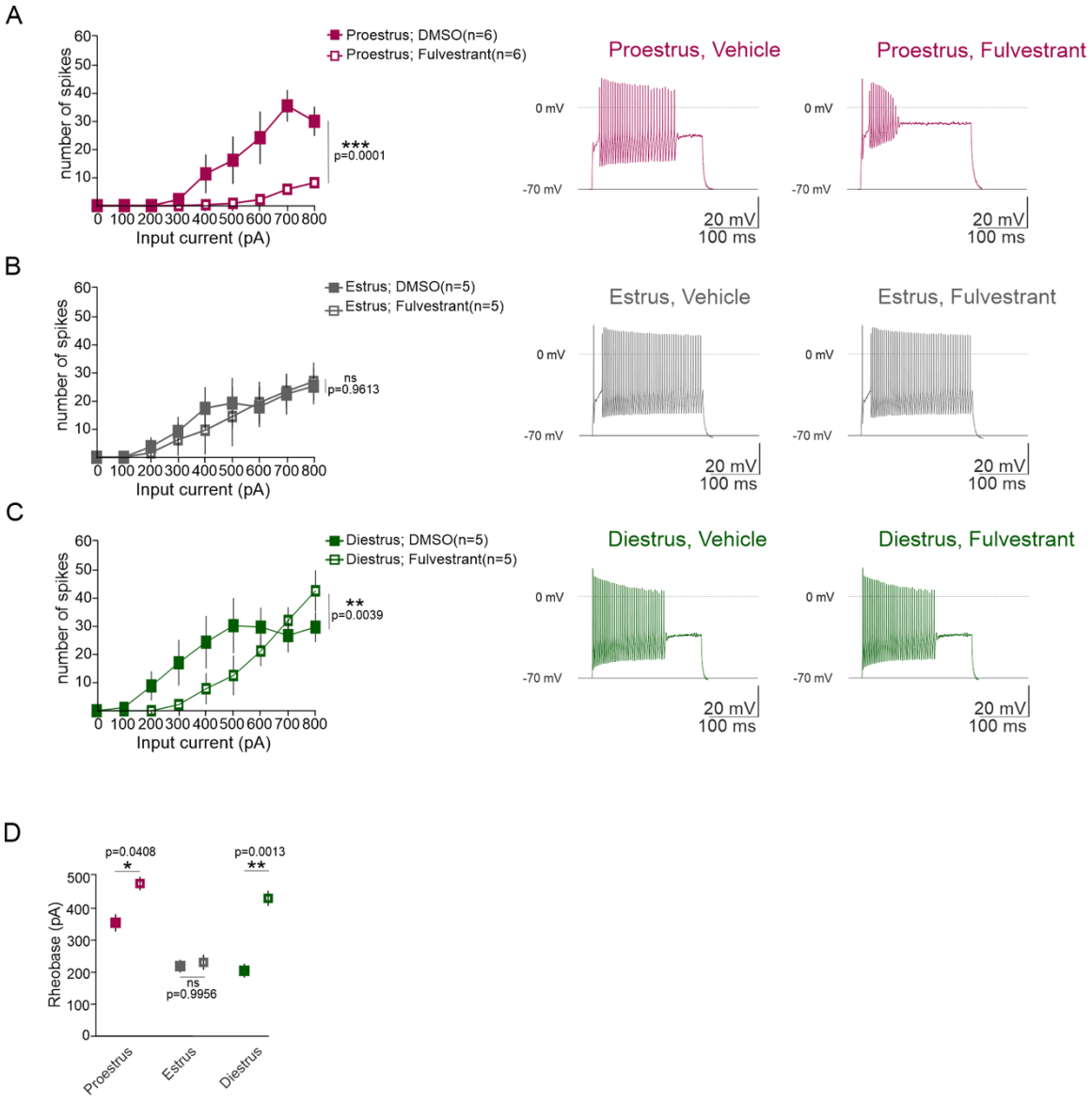

Figure 19. Fulvestrant effect on FSIs active properties across estrous phases. (A)(Left) *Time course of the number of action potential evoked by a series of depolarizing current injections in proestrus phase before and after bath application of Fulvestrant.* ***(Right)*** *Representative traces of voltage responses in proestrus female FSIs to a step of depolarizing current injection of 300 pA f before and after bath application of Fulvestrant.* ***(B) (Left)*** *Time course of the number of action potential evoked by a series of depolarizing current injections in estrus phase before and after bath application of Fulvestrant.* ***(Right)*** *Representative traces of voltage responses in estrus female FSIs to a step of depolarizing current injection of 300 pA before and after bath application of Fulvestrant.* ***(C) (Left)*** *Time course of the number of action potential evoked by a series of*

depolarizing current injections in diestrus phase before and after bath application of Fulvestrant. ***(Right)*** *Representative traces of voltage responses in diestrus female FSIs to a step of depolarizing current injection of 300 pA before and after bath application of Fulvestrant.* ***(D)*** *Box plots summarizing average values of rheobase pre and post bath application of Fulvestrant [Proestrus: n=6, mice =4, vehicle 355 ± 29.41 pA vs treatment 478.3 ± 18.33 pA, *p=0.0408; Sidak. Estrus: n=5; mice =4, vehicle 216 ± 24.41 pA vs treatment 226 ± 28.74 pA, p=0.9956; Sidak. Diestrus: n=5; mice = 4, vehicle 202 ± 38.91 pA vs treatment 424 ± 35.58 pA, **p=0.0013; Sidak]*.

In-vivo FSIs activation following thalamic glutamatergic input stimulation differs by sex and estrous cycle phase.

So far, our results indicate that sex and estrous cycle phase influence FSIs responsiveness to excitatory thalamic input as well as neuronal intrinsic excitaiblty. To establish whether this modulation ultimately shapes thalamic-induced activation of FSIs *in-vivo*, we took advantage of fiber photometry experiments coupled with optogenetics.

In male and female Pv-CRE mice, we virally expressed the AAV5-hSyn-ChrimsonR-tdTomato in Pf, the green, fluorescent genetically encoded calcium indicator AAV9-DIO-GCamp8m in the DLS (*Zhang et al., 2021*) and implanted an optical fiber in the DLS. Four weeks after surgery, mice were placed in an open field (OF) arena for five consecutive days before the fiber photometry experiments. Since the OF test is used to assess locomotor activity and anxiety-like behavior (*Liebsch et al., 1998*), this habituation period of five days was needed to ensure the absence of stress from our recordings. On the sixth day, we performed combined optogenetic and fiber photometry experiments to collect bulk calcium signals from FSI ensembles in freely behaving mice (**Fig.20A**).

To optogenetically activate Pf terminals in the DLS, we applied 20 ms square pulses at 1 mW/mm^2 laser power and 40 Hz, a frequency that is sufficiently fast to reveal dynamic properties while remaining within the activation/inactivation range of ChrimsonR (*Klapoetke et al., 2013*). By measuring the area under the curve (A.U.C.) upon optogenetic stimulation of Pf fibers in the striatum, we observed a main effect of sex and estrous cycle fluctuation *[A.U.C. Sex and estrous cycle: $F1.963_{,17.66}=0.7067$; DF=3; p=0.5042, Tukey;*

stimulation: F3,9=24.63, DF=3; p=0.0001; Tukey; Sex andestrous cycle X stimulation: F9,27=4.870; DF=9; p=0.0006; Tukey].

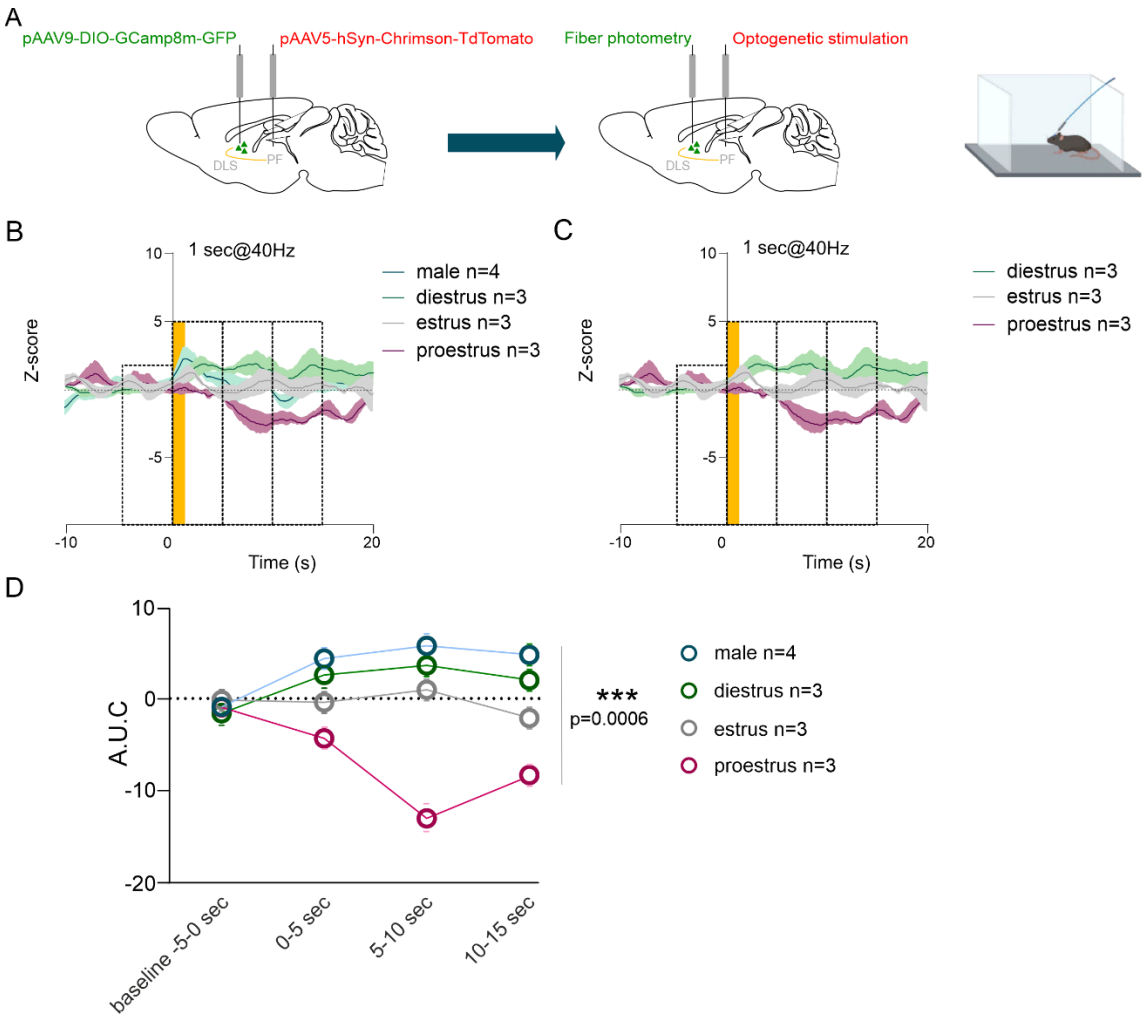

Figure 20. In-vivo FSI activity following thalamic optogenetic stimulation ***(A)*** *(Left) Schematic of AAV5-hSyn-Chrimson.TdTomato injection in the PF and* AAV9-DIO-GCamp8m-GFP *in the DLS, optic fiber implantation in the DLS. (Right) Schematic representing a mouse placed in an open field arena.* ***(B-C)*** *(Left) Z-score time course of optogenetically stimulated GCamp8m fluorescence. The highlighted zone (yellow rectangle) represents the duration of the optogenetic stimulation (1 second), while the black rectangles represent the time range considered for the A.U.C. analysis: baseline (5s), stimulation (5-10-15s)* ***(D)*** *Time course of the A.U.C. during 5 seconds of baseline and at different time points after the stimulation. Each dot represents the average of all the mice per group.*

In the 15 seconds following Pf terminals stimulation, we observed a significant increase in GCamp8m fluorescence in both males (**Fig. 21A**) and diestrus phase females (**Fig. 21B**) compared to baseline, while no differences were detected in estrus phase females (**Fig. 21C**). In contrast, in proestrus phase females we observed a decrease of calcium signal 5 to 10 seconds after thalamic stimulation (**Fig. 21D**).

Comparing males and the three *estrous* phases, we found a significant difference between males and proestrus phase females *[A.U.C. male vs proestrus: $F_{1,5}$=50.39; DF=1; p=0.0009, Tukey; stimulation: $F_{3,15}$=1.486, DF=3; p=0.2586; Tukey; stimulation X male vs proestrus: $F_{3,15=}$9.525; DF=3; p=0.0009; Tukey]* (**Fig. 20D**).

Within estrous phases GCamp8m-GFP fluorescence was generally reduced following optogenetic stimulation during the proestrus and then progressively increased following the estrous cycle (**Fig.21 C-D**), possibly reflecting cycle-related fluctuations in estradiol and progesterone plasma levels. Moreover, we found that diestrus phase females significantly differ from both proestrus [*A.U.C. proestrus vs diestrus: $F_{1,4}$=92.46; DF=1; p=0.0007, Tukey; stimulation: $F1_{.489,5.958}$=3.641, DF=3; p=0.0987; Tukey; stimulation X proestrus vs diestrus: $F_{3,12=}$14.98; DF=3; p=0.0002; Tukey*] and estrus phase female [*A.U.C. proestrus vs estrus: $F_{1,4}$=29.91; DF=1; p=0.0054, Tukey; stimulation: $F_{1.425,5.702}$=5.007, DF=3; p=0.0622; Tukey; stimulation X proestrus vs estrus: $F_{3,12=}$6.177; DF=3; p=0.0088; Tukey*]. These preliminary results indicate that glutamatergic inputs from the thalamus are differently processed by striatal FSI ensembles in a sex and estrous phase-dependent manner.

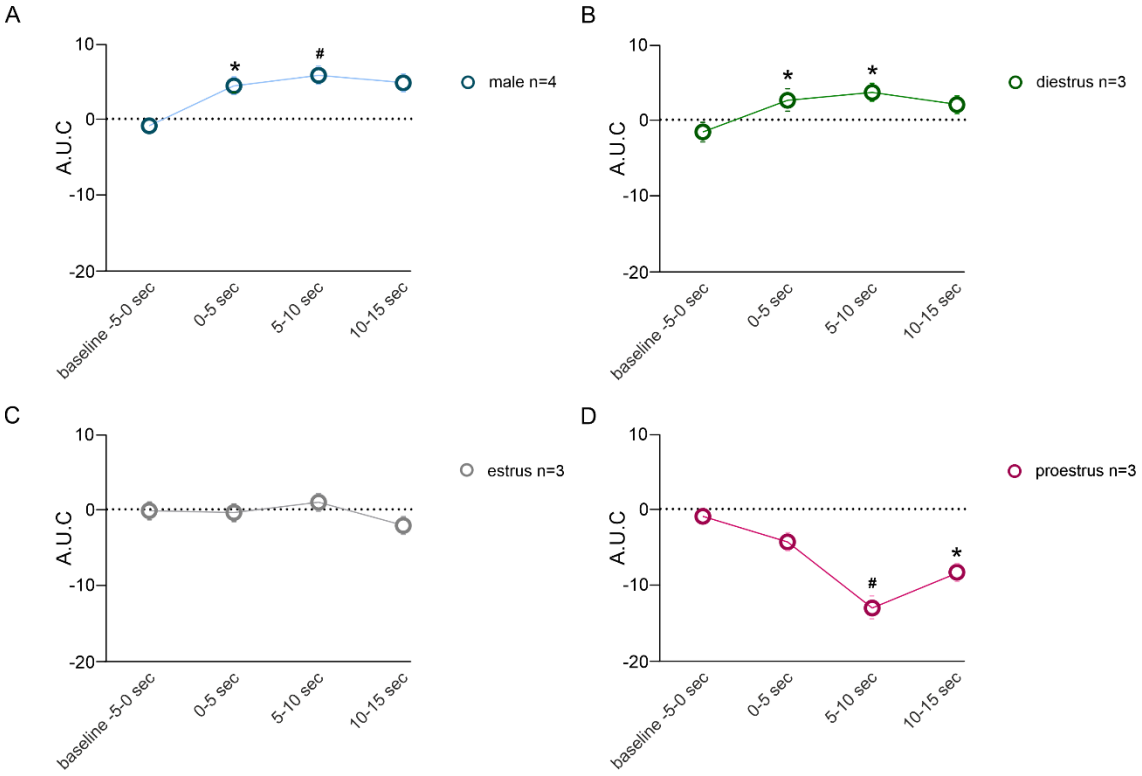

Figure 21. In-vivo FSI activity following thalamic optogenetic stimulation in the single groups. ***A-D*** *Time course of the A.U.C. during 5 seconds of baseline at different time points after the stimulation. Each dot represents the average of all the mice per group.*

Project Implementation

Our study's key findings can be summarized as follows:

1) DLS FSIs integrate thalamic excitatory input differently depending on sex and estrous phase, both ex vivo and in vivo.

2) Sex and estrous phases impact the active properties of FSIs, which are likely linked to neuronal firing activity and synaptic responsiveness, leaving unaffected passive properties.

3) Pharmacological manipulation of estrogen-mediated signaling exacerbates differences in FSI excitability in proestrus and diestrus phase
Thus, whereas sex and hormonal conditions alter FSI processing of thalamic inputs, the underlying mechanisms are unlikely to be primarily dependent on estrogen receptor pathways.

Our future experiments aim at:

- assessing progesterone interplay in shaping FSI responsiveness to thalamic glutamatergic stimuli and excitability.
- examining the potential involvement of Calcium activated K channels BK and SK in modulating FSI excitability across estrous cycle in females.
- establishing whether and how gonadal hormones interact with the neuromodulator 5-HT released from dorsal raphe nucleus (DRN).

Assessing progesterone interplay in shaping FSI responsiveness to thalamic glutamatergic stimuli and excitability

The female estrous cycle is characterized by cyclical changes not only in estradiol but also in other hormones such as progesterone. Although estradiol and progesterone action trigger distinct processes, the combination of both is necessary for the expression of the many behaviors, among which the ones mediated by striatum (*Proaño et al., 2018; 2020, 2023; Morisette et al., 1990*).

In NAc SPNs, circulating levels of estradiol and progesterone together correlate with changes in synaptic and active cell properties during proestrus, suggesting a synergistic action (*Proano et al., 2020, 2023*). Based on this evidence we hypothesized that the reduction in excitatory synaptic integration and excitability observed in DLS-FSIs during the proestrus phase may be mediated by an integrated, rapid progesterone action, in addition to the acute estradiol action discussed above *(see "Discussion"*). Thus, an important future direction for this line of research would be to test the possible interplay of progesterone in shaping FSI responsiveness to thalamic input and intrinsic excitability. Those experiments will be performed in the presence of progesterone, and across different estrous cycle phases.

A second cohort of female mice will be studies to assess the progesterone influence on active and passive FSI properties.

Examining the potential involvement of Calcium activated K channels BK and SK in modulating FSI excitability across estrous cycle in females

Estradiol and progesterone interaction with large conductance (BK) and small conductance (SK) Ca^{2+} -activated K^{+} channels BK and Small conductance (SK) have been reported in many tissues (*Valverde et al., 1999; Coiret et al., 2005; North et al., 2023; Kelly et al., 1999, 2003*). Since BK and SK are fundamental regulators of neuronal excitability, participating in determining inter-spike interval and spike-frequency adaptation *(Vergara et al., 2018.)* Calcium-activated potassium channels likely play a key role in synaptic transmission (*Tazerart et al., 2022*). Following an increase in intracellular calcium ions, they prolonged afterhyperpolarization (AHP), resulting in an augmented inter-spike interval and in a general hyperpolarizing influence when activated (*Bond et al., 2005*). This reduction in membrane potential influences how readily a neuron integrate post synaptic depolarization and ultimately it fires in response to incoming stimuli (*Vergara et al., 2004*). We hypothesize that the observed sensitivity of striatal FSI excitability to the estrous cycle in females could be a consequence of estradiol and progesterone interaction with these calcium-activated potassium channels *(see "Discussion*").To test the possibility, we will perform whole-cell patch clamp experiments in PV-Cre females. The role of BK channels in shaping FSI excitability will be assessed by using the BK channel blockers iberiotoxin

(*Galvez et al., 1990*), while SK will be isolated from other currents by bath application of SK channel blocker apamin (*Herrera et al., 2002*).

Establishing whether and how gonadal hormones interact with the DRN-released 5-HT

The serotonergic system is a main target of ovarian hormones, which affect the generation and efficacy of serotonergic neurotransmission (*McEwen, 2002; Bethea and Reddy, 2012*). Estrogen has been reported to have potent serotonin-modulating properties acting at different levels from neurotransmitter synthesis, through the regulation of the enzyme tryptophan hydroxylase (*Lu et al., 1999*), and degradation of 5-HT to the density and binding of 5-HT receptors (*Bethea et al., 2002*). The effect of estrogen on the temporal-dynamics release of serotonin seems to depend on several factors such as receptors subtype and brain area. For instance, 5-HT1B autoreceptor mRNA (*Hiroi and Neumaier, 2009*), and MAO-A mRNA and activity (*Gundlah et al., 2002*) in the dorsal raphe nucleus (DRN) are decreased after estrogen treatment, while estrogen administration has been found to increase 5-HT2A mRNA levels in brain areas relevant for the control of mood, mental state and cognition (*Sumner and Fink, 1998*).

Besides estrogen, progesterone has been suggested to increase serotonergic neurotransmission via the regulation of the expression of serotonin-related genes and proteins (*Bethea et al., 2002; Smith et al., 2004; Sanchez et al., 2005*). Chronic progesterone treatment seems to decrease 5-HT1A receptor expression in rats (*Biegon et al., 1983*). All together, these findings point to an interaction between ovarian hormones and serotonergic activity in females.

To test whether serotonin levels differ across estrous cycle phases within the DLS, female PV-Cre mice will be injected at the level of the DRN, the main source of 5-HT for the dorsal striatum (*Ren et al., 2018*), with a viral vector bearing an hM3Dq Designer Receptors Exclusively Activated by Designer Drugs (DREADD) excitatory construct (AAV-hM3Dq). Mice will be also injected in the striatum with the serotonin sensor AAV9-hSyn-HT3.5. On ex-vivo DLS slices, we will apply deschloroclozapine (DCZ, the selective agonist of DREADD-hM3Dq). This experimental approach will allow us to evaluate the different levels of DRN released 5-HT across female estrous phases.

We validated the functionality of the serotonin sensor 5-HT3.5 performing preliminary ex-vivo experiments in females PV-Cre. Bath application of exogenous 5-HT (0.5mM) resulted in a significant increase in 5-HT3.5 fluorescence signal (**Fig 22**).

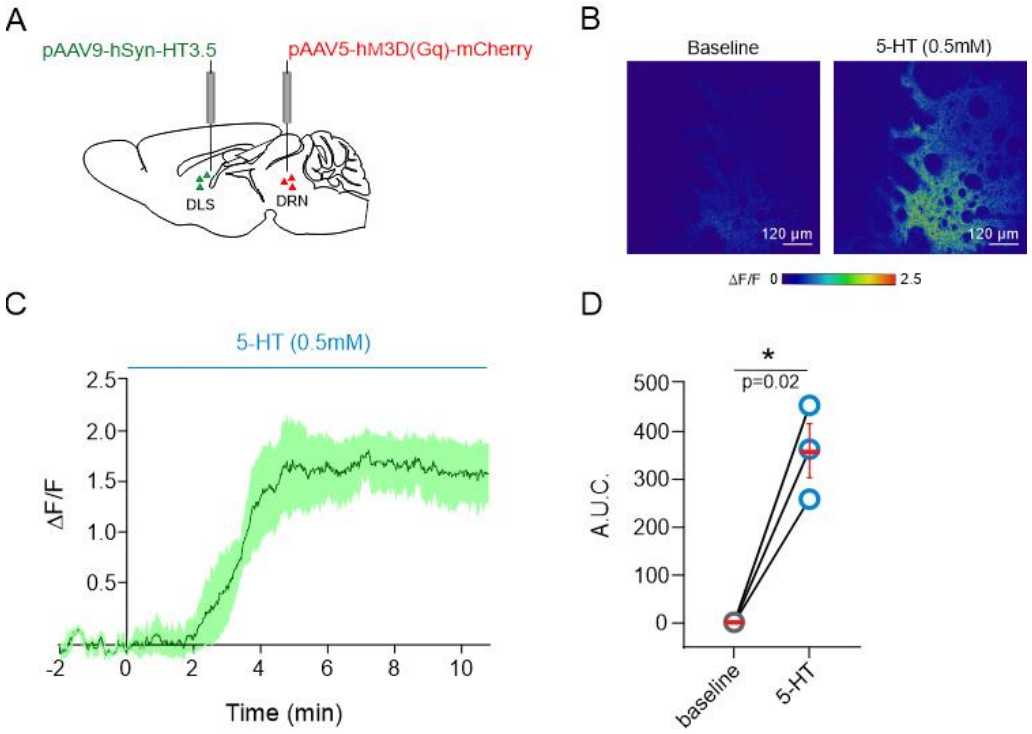

Figure 22. Ex-vivo validation of the 5HT3.5 sensor. (A) *Experimental design. Schematic of HT3.5 sensor injection in DLS and hM3D (Gq)-mCherry in DRN.* ***(B)*** *Representative images of ex-vivo DLS slices in baseline condition and following 5-HT (0.5 mM) application.* ***(C)*** *Z-score time course of 5-HT stimulated 5-HT3.5 fluorescence.* ***(D)*** *Scatter plot of the A.U.C. during baseline (2 min) and during the bath-application of 5-HT (8 min) [baseline: n=3; 0.01535 ± 0.0195; 5-HT: n=3; 358.7± 56.39; baseline vs5-HT *p=0.02; 2tailed unpaired t-test, t=6.362, df=2]. Values are expressed as mean ± SEM.*

Further on, we aim to investigate the possible influence of 5-HT on striatal FSIs responsiveness to thalamic input in relation to estrous cycle hormones. To assess this, female PV-Cre mice will be double injected in Pf with the fast channelrhodopsin Chronos (pAAV5-Syn-Chronos-GFP) and in striatum and at the level of the DRN with the viral vector AAV-hM3Dq. We will then perform *ex-vivo* optogenetic experiments, as described

in **Fig. 11 "Results"**, in upon systemic injection of DCZ (**Fig.23).** This experimental approach will allow us to investigate the role of 5-HT in modulating the responsiveness of FSI to excitatory glutamatergic stimuli.

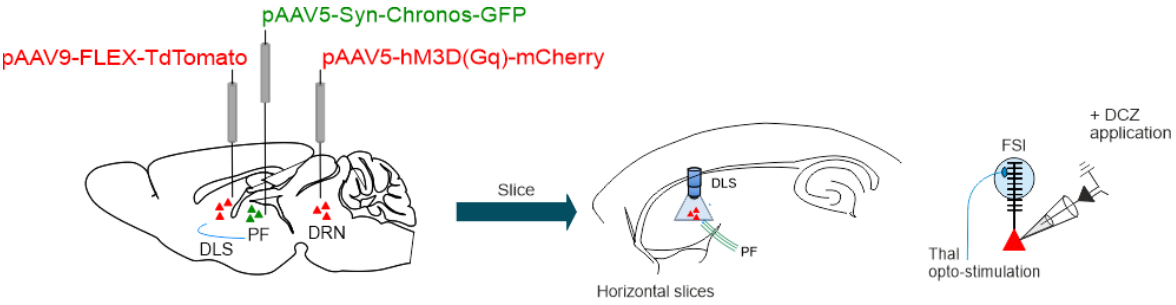

Figure 23. Schematic representation of experimental setting. *Schematic of FLEX-TdTomato injection in DLS and Chronos-GFP in PF, and injection of hM3D(Gq)-mCherry in DRN, and recording configuration.*

Additional project

In collaboration with Massimo Pasqualetti and Alessandro Gozzi, we validated two viral vectors that alter AMPAr subunits either promoting or inhibiting receptor insertion in the cell membrane.

The two constructs were tested in male C57BL/6 mice, taking advantage of the well-studied cortex-SPN synapse. Mice were bilaterally injected in primary motor cortex M1 with red-light drivable channelrhodopsin AAV5-Syn-ChrimsonR-tdTomato.Two weeks after, mice were then injected in DLS with constructs that express either the AMPA receptor subunit GluR4 (AAV8-Tet-GFP-GluR4), which undergoes synaptic delivery and increases synaptic transmission under basal conditions, or the C-terminus of GluR4 (AAV8-Tet-RFP-R4Ct) which can block synaptic trafficking of AMPA receptors. The two viruses were injected together with the transactivator tTA (1:1 transactivator:construct), which is an artificially designed potent transcription factor. The bind between the transactivator tTA and the Tet responsive promoter (present on the two constructs) is controlled by the chemical inducer doxycycline (Dox). For this reason, in experimental mice, two weeks after viral injections we performed five consecutive days of single intraperitoneal injection of Dox (50 μg/g) for gene expression induction. On the sixth day, on ex-vivo DLS brain slices, we recorded EPSCs evoked by a single blue light pulse through the microscope objective (1 ms at 470 nm) in either RFP^+ or GFP^+ SPNs. Whole-cell patch clamp technique was used to measure SPN AMPA/NMDA ratio upon optogenetic stimulation of cortico-striatal projections (**Fig. 24**).

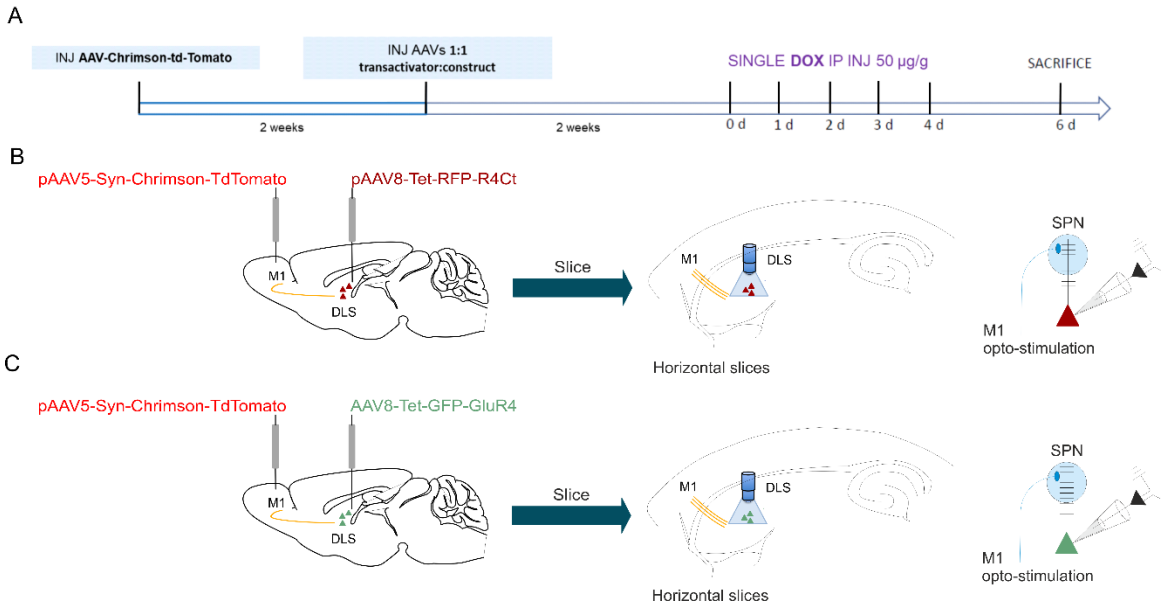

Figure 24. Schematic representation of experimental setting. (A) *Schematics illustrating the pharmacological and electrophysiological regime.* ***(B)*** *Schematic of AAV5-hSyn-Chrimson-TdTomato injection in M1, and AAV8-Tet-RFP-R4Ct in the DLS.* ***(C)*** *Schematic of AAV5-hSyn-Chrimson-TdTomato injection in M1, and AAV8-Tet-GFP-GluR4 in the DLS.*

The measured AMPA/NMDA ratio was compared with a control group in which the cerebral injection of either AAV8-Tet-GFP-GluR4 or AAV8-Tet-RFP-R4Ct was not followed by Dox treatment, preventing the gene expression of the constructs. We observed a significant reduction in AMPA/NMDA ratio in SPNs infected with R4Ct construct upon Dox-induced expression in comparison with the control group without Dox treatment (control vs treatment, p=0.219) (**Fig. 25A**). Conversely, we observed a significant increase in AMPA/NMDA ratio in SPNs infected with Glur4 construct upon Dox-induced expression in comparison with the control group without Dox treatment. (**Fig. 25A**) For both constructs, this alteration was likely due to a modification in AMPA-mediated EPSC amplitude since no significant changes were detected in NMDA-mediated EPSC (**Fig. 25B**). Our electrophysiological data validate the functionality of the two constructs.

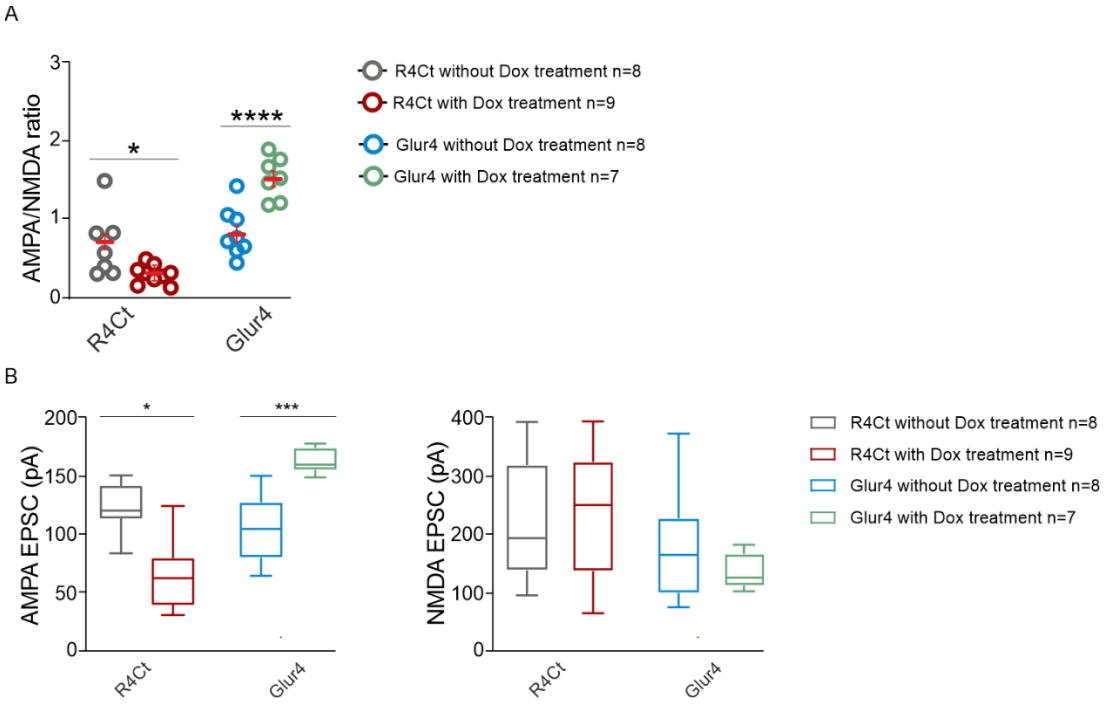

Figure 25. AMPA/NMDA ratio between males and females across estral phases (A) *AMPA/NMDA ratio in R4Ct and Glur4 infected cells. (AMPA AMPA/NMDA ratio, R4Ct: without DOX cells=8; mice= 5; 0.6724 ± 0.1580; with DOX treatment: cells=9; mice= 7; 0.2988 ± 0.039 pA;) (AMPA/NMDA ratio, Glur4: without DOX cells=8; mice= 6; 0.8204 ± 0.1102; with DOX treatment: cells=7; mice= 5; 1.518 ± 0.1015) Values are expressed as mean ± SEM.* ***(B)*** *(Left) Box plots representing AMPA and (right) NMDA -mediated current (pA) in R4Ct and Glur4 infected cells. Box plot extends from the 25th to the 75th percentile, whiskers extend from the minum to the maximum, the line in the middle of the box shows the median value. (AMPA, R4Ct: without DOX cells=8; mice= 5; 123.6 ± 8.286 pA; with DOX treatment: cells=9; mice= 7; 62.25 ± 14.49 pA; Glur4: without DOX cells=8; mice= 6; 129.5 ± 12.70 pA; with DOX treatment: cells=7; mice= 5; 201.3 ±4.969 pA) (NMDA, R4Ct: without DOX cells=8; mice= 5; 231.3 ± 39.88 pA; with DOX treatment: cells=9; mice= 7;2 454.3 ± 45.43 pA; Glur4: without DOX cells=8; mice= 6; 181.5 ± 37.71 pA; with DOX treatment: cells=7; mice= 5; 201.3 ± 11.10 pA).*

Discussion

Naturally occurring hormone cycles in adult female humans and rodents create a dynamic neuroendocrine environment with potential influence on brain function (*Breedlove and Arnold 1981; Cahill 2014; Gorski 198*5). One class of behaviors sensitive to cycle-related hormonal fluctuations include those related to reward-seeking and motivation. Consequently, sex hormones profoundly affect disorders such as depression and addiction (*Baran et al. 2009, 2010; Becker et al. 2001, 2012; Becker and Hu 2008; Jackson et al. 2006, Lebron-Milad and Milad 2012; Milad et al. 2009; Walf and Frye 2006*). Investigations into the neural substrates instrumental for these behaviors and disorders have targeted striatal brain regions (*Proano et al., 2017*). Though striatal-related behaviors and pathologies display clear sex dimorphism, the mechanisms by which sex and gonadal hormones influence striatal physiology remain largely unknown (*Meitzen et al., 2018*). Besides the direct action on SPNs through membrane and nuclear receptors, sex hormones have been proposed to act also on striatal interneurons, which in turn synapse upon SPNs (*Krentzel & Meitzen, 2018a*). The relationship between striatal interneurons and sex hormones has been investigated only from a behavioral point of view. In 2017, Rapanelli and colleagues demonstrated that FSI specific disruption in the dorsal striatum of mice is sufficient to produce behavioral abnormalities characteristic of autism spectrum disorder (ASD) and Tourette syndrome (TS). Interestingly, these were apparent in male but not in female mice, with consequent aberrant molecular signaling in SPN activity (*Rapanelli et al., 2017*). FSI exerts a coordinated role in intrastriatal information processing and upon synchronous activation, they can convert an input signal into a GABAergic inhibitory output signal, shaping in turn SPN activity to downstream basal ganglia nuclei (*Berke, 2008*). A major source of excitatory input to the striatal network is from the thalamic nuclei (*Aoki et al., 2015*), among which the Pf nucleus constitutes the major source of thalamostriatal connections in rodents (*Galvan and Smith 2011*). Pf fibers make stronger excitatory connections onto FSIs than onto other striatal cells, leading to the idea that excitatory glutamatergic inputs from Pf are shaping striatal network activity by strongly influencing FSIs´ input encoding (*Johansson & Silberberg, 2020*).

Therefore, understanding the influence of sex hormones and the estrous cycle on FSI processing of thalamic input could be instrumental in explaining sex differences in striatal-mediated behavior and the relevant disorders.

Ex vivo FSI synaptic responsiveness to thalamic glutamatergic input

We initially examined how the estrous cycle and sex hormones influence the Pf-FSI synapse. By performing ex-vivo electrophysiological recordings in mice, we demonstrated that FSIs have distinct synaptic efficacy during optogenetic thalamic stimulation between sexes and within estrous cycle phases (**Fig. 12**). Our study is, to the best of our knowledge, the first to provide evidence of a sex-dependent modulation of synaptic processing on striatal FSIs. Previous studies focused on sex-dependent regulation of SPN neuronal transmission in the NAc and CPu. In the NAc, SPNs exhibit robust changes in the strength of non-input-specific excitatory glutamatergic neuronal transmission, as measured by miniature excitatory postsynaptic currents (mEPSCs) across estrous cycle phases. No differences in mEPSC properties were detected across estrous cycle phases in CPu, suggesting that baseline glutamatergic inputs in SPNs of CPu are not as sensitive to the estrous cycle as their counterparts in the NAc (*Proano et al., 2023*). Our results possibly suggest that the synaptic temporal integration of input-specific thalamic stimuli at the DLS-FSI level is sensitive to sex hormones; however, we cannot yet rule out that alternative sex hormone-dependent adaptations occur at other FSIs´ inputs.

Notably, we observed a progressive increase in synaptic responsiveness within estrous phases (**Fig. 12**), which seems to correlate with cycle-related hormonal fluctuations (*Proano et al., 2020*) and cycle-related peaks in estradiol and progesterone plasma levels occurring during the proestrus phase. The reduced synaptic efficacy to thalamic stimuli depicted in FSI during the proestrus phase could be the consequence of the peak in estrogen plasma levels occurring at the beginning of this estrous phase, together with the following progesterone peak. Although estradiol and progesterone action trigger distinct processes, the combination of both is necessary for the expression of behaviors, such as the mating one (*Proano et al., 2023*) and interactions have been reported in many brain areas (*Baudri et al.. 2013*), including the NAc (*Proano et al., 2020*). Electrophysiological data on NAc SPNs showed a correlation between circulating levels of estradiol and progesterone and

mEPSC frequency (*Proano et al., 2020*). Proano and colleagues proposed that the prominent decrease in excitatory synaptic properties, assessed as mEPSC frequency in the proestrus phase only and not observed in any other estrous cycle phase, might be mediated by rapid progesterone action, in addition to the acute estradiol effect (*Proano et al., 2020*). We propose that this synergistic action and counter-regulatory effect of both types of ovarian hormones might be crucial for DLS-FSIs functioning, therefore affecting FSI integration of synaptic inputs. Further experiments will be needed to evaluate this hypothesis (*see "Project implementation"*).

According to Proano and colleagues´ recent review (*Proano et al., 2023*), ovarian hormones, such as estradiol, can modulate glutamatergic transmission and shape glutamate release probability in NAc SPNs through the ERs expressed on presynaptic terminals. Immunohistochemical staining also revealed the potential presynaptic site of action of estrogen. Staining in rats showed the expression of estrogen receptors at axons and presynaptic terminals of the thalamus (*Mitra et al., 2003*), suggesting that estrogen can potentially shape glutamate release at thalamo-striatal synapses. Nevertheless, functional studies showing how estrogen can modulate the thalamo-striatal connection, and specific investigations on Pf-striatal projecting fibers have not been performed yet.

To check the potential effects of sex hormones at the Pf-FSI presynaptic site, in our experiments, we analyzed the paired-pulse ratio (PPR), a hallmark of presynaptic plasticity frequently used as a measure of the neurotransmitter release probability (*Manabe et al., 1993, Debanne et al., 1996, Dobrunz and Stevens, 1997*). We did not observe any difference in PPR across sex nor female estrous phases (**Fig. 13B**), pointing against a primary presynaptic site of action of sex hormones in the regulation of Pf-FSI connection. We therefore hypothesized that sex hormones, instead of acting presynaptically, could act postsynaptically at the Pf-FSI synapse to regulate its strength. In the NAc, membrane estrogen receptors are expressed both on SPN somas and dendritic spines (*Almey et al., 2012, 2015, 2016*), suggesting that estrogen can directly act postsynaptically, eventually shaping glutamatergic neuronal transmission. In Cyr and colleagues´ review (*Cyr et al., 2001*), ovarian steroids have been reported to modulate striatal SPN NMDA and AMPA receptors. Specifically, in ovariectomized rats, estradiol treatment induced a reduction in

AMPA and NMDA receptor binding in the striatum, while no effect was reported after progesterone treatment. Therefore, we decided to test whether the differences we observed in FSI temporal integration of Pf inputs could be the result of sex hormones interaction on postsynaptic AMPA and NMDA receptors. In our experiments, the AMPA/NMDA ratio was not different between experimental groups (**Fig. 14B**), suggesting that sex and estrous phases are not shaping the availability nor the proportion of the two main glutamatergic ionotropic receptors.

Besides ionotropic receptors, estrogen receptors are known to activate also metabotropic glutamate receptors (mGluRs). In vivo and ex vivo experiments demonstrated that estrogen receptors locatedin the membrane with metabotropic glutamate receptors are involved in drug addiction (*Tonn Eisinger et al., 2018*), facilitate locomotor sensitization to cocaine (*Martinez et al., 2014*), and alter dendritic spine density in the rat NAc (*Peterson et al., 2015*). For instance, in gonadectomized female rats, Mermelstein and colleagues showed that estradiol administration induces changes in spine attributes, such as size and density, acting through a membrane estrogen receptor associated with mGluR5 on NAc SPNs (*Gross et al., 2016; Peterson et al., 2015a, 2016*). This pathway has been proposed to also mediate the changes in spine attributes observed by Beeson and Meitzen (*Beeson and Meitzen, 2022*) in NAc SPNs of gonad-intact females. In their work, the authors demonstrated that the estrous cycle can impact dendritic spine plasticity highlighting a possible neuroanatomical mechanism linking dendritic spine changes and electrophysiological data from other work. In this context, the rapid reduction in spine size observed during the proestrus phase could be a consequence of estradiol and progesterone peaks, which leads to a decrease in the number of available synapses and therefore a decrease in mEPSC frequency observed in other electrophysiological experiments (*Beeson and Meitzen, 2022; Proano et al., 2023*). Consistent with this conclusion, they observed similar spine attributes in males and females in the diestrus phase, during which estradiol and progesterone plasma levels are at a minimum (*Beeson and Meitzen, 2022;* Proano et al., 2020). This observation also correlates to electrophysiological data indicating that NAc SPNs properties from females in the diestrus phase are similar to males, unlike SPNs recorded during other estrous cycle phases (*Beeson and Meitzen, 2022; Proaño et al., 2018, 2020*). The contribution of testosterone to the modulation of glutamatergic input into the

striatum is less well known (*Proano et al., 2023*). Though the body of literature is gradually growing, evidence so far indicates that exposure to systemic testosterone and/or its metabolite dihydrotestosterone at various doses can regulate dendritic spine density and morphology in the NAc in either castrated or gonad-intact male rats (*Tobiansky et al., 2018*). This androgenic action appears to be mediated via mGluR5 activity, similarly to estradiol (*Gross et al., 2018*).

We speculate that the differences in synaptic temporal integration across sex and estrous phases observed at the Pf-FSI synapse could be mediated by multiple mechanisms, among which gonadal hormones action on FSI spines attributes, possibly through an interaction with mGluRs.

Ex vivo FSIs intrinsic excitability

Electrophysiological recordings of NAc activity showed that the intrinsic excitability properties of SPNs robustly change across the estrous cycle (*Proano et al., 2018*). Besides SPNs, we still lack evidence of a rapid modulatory effect of gonadal hormones on the intrinsic excitability of other striatal neurons. Our whole-cell patch clamp experiments (**Fig. 15-16**) indicate that FSI intrinsic neuronal excitability is increased in males compared to females. These findings are in line with evidence positing that estradiol leads to a decrease in striatal SPN neuronal excitation by binding to membrane estrogen receptors (*Yoest et al., 2014, 2018*). Estradiol action on striatal SPNs may be mediated by several membrane-associated estrogen receptors, as the NAc and other striatal regions are known to express ERs α, β, and GPER-1 with sparse or no expression of nuclear receptors in adult animals (*Almey et al.,2012, Almey et al.,2015*).

Through non-genomic action on membrane-associated estrogen receptors, estradiol has been proposed to act on L-type calcium currents in the striatum, consequently modulating changes in cell excitability (*Grove Strawser et al, 2010, Mermelstein et al, 1996*). In acutely dissociated and cultured rat neostriatal neurons, estradiol was found to reduce Ba2+ entry reversibly via L-type Ca2+ channels in a sex-specific manner, as the reduction of Ba2+ currents was greater in neurons taken from female rats (*Mermelstein et al, 1996*). Moreover, in female rat striatal neurons, membrane-localized ERα and ERβ have been reported to activate metabotropic glutamate receptors mGluR3 to attenuate L-type calcium

channel-dependent CREB signaling, resulting in an inhibition of L-type calcium channel currents (*Strawser et al, 2010*). Besides estradiol, progesterone has also been reported to interact with L-type calcium channels, blocking calcium entry and leading to alterations in the signaling of the activity-dependent transcription factors NFAT and CREB. The reduction in Ca^{2+} influx following gonadal hormone interaction can in turn affect calcium-activated potassium channels, such as BK and SK channels (*Luoma et al., 2011*).

Besides the receptor-mediated action, large-conductance Ca^{2+} and voltage-activated K^{+} (BK) channels have been reported to be directly modulated by estradiol binding to the four β regulatory subunits (*Valverde et al., 1999*), but the results are diverse and conflicting depending on doses of estrogen and the tissue orcells used (*Coiret et al., 2005*). Also, progesterone, already at micromolar doses (≥1 μM) has been reported to activate mouse cerebrovascular myocyte BK channels, interacting with β regulatory subunits (*North et al., 2023*). In neurons of the hypothalamus, transient estrogen exposure induced enhancement of the coupling of α-adrenergic receptors to their effector SK channels, leading to inhibition of the SK current in these GABAergic neurons (*Kelly et al., 2003*). The same effect has been reported in CA1 hippocampal neurons, where estradiol exposure rapidly augments α-adrenergic inhibition of SK channel activity (*Kelly et al., 1999*).

Since BK and SK are fundamental regulators of neuronal excitability, participating in determining inter-spike interval and spike-frequency adaptation *(Vergara et al., 2018),* we speculate that the observed sensitivity of striatal FSI excitability to the estrous cycle could be a consequence of estradiol and progesterone interaction with these calcium-activated potassium channels. Further experiments would be needed to test this hypothesis (see "Project implementation").

Pharmacological manipulation of estrogen-mediated signaling exacerbates differences in FSI excitability in proestrus and diestrus phase

As discussed above, the growing body of work in this subject strongly suggests that estrogen could rapidly modulate cell intrinsic excitability acting on membrane estrogen receptors such as GPER, membrane-associated ERα, and membrane-associated ERβ (*Krentzel et al. 2018*). Therefore, as a first step to elucidate the specific mechanisms behind the changes in FSI excitability observed across estrous phases, we exploited the use of

antiestrogen compound Fulvestrant in striatal slices of female brains. Fulvestrant application failed to rescue excitability differences across estrous phases, inducing changes in FSI excitability in proestrus and diestrus phases only while no effect was detected during the estrus phase (**Fig. 18-19**). As discussed above, data in the literature indicates that the proestrus phase is characterized by a peak in estradiol levels first followed by a progesterone surge. Plasma levels of estradiol and progesterone slowly decrease during the following estrus phase although some effects can still be present in tissues and remain relatively low in the diestrus phase (*Proano et al., 2017, 2023*). We therefore proposed that the interaction and balanced effect of both types of ovarian hormones might be crucial for normal functioning of FSIs, leading to changes in FSI excitability across estrous phases. Application of Fulvestrant disrupts this balance reducing estrogen receptor recruitment relative to progesterone. This unopposed action of progesterone could explain the observed exacerbation of excitability differences.

Interestingly, Fulvestrant, a drug widely used in the clinic for the treatment of metastatic breast cancer (*Wardell et al.,* 2020) exhibits an inhibitory effect on the excitability of a crucially positioned class of striatal interneurons. This effect might be potentially important from a translational point of view.

Our ex-vivo data underscore the complexity of estrous cycle influences and suggest that a reduction in excitability evoked by Fulvestrant action in the proestrus and diestrus phases only, is mediated by multiple mechanisms. For instance, investigations in the hippocampus report a differential expression and distribution of membrane-associated ERα and ERβ across the estrous cycle (*Mendoza et al., 2019*). Although a similar characterization in the striatum across estrous cycle phases has not been performed.One possibility is that estrogen membrane receptor expression could change across the estrous cycle, possibly explaining the ability of Fulvestrant to differentially affect the estrous cycle phases.

In vivo FSI neuronal activation in response to thalamic input stimulation

To establish whether modulation of sex hormones shapes thalamic-induced activation of FSIs *in-vivo*, we took advantage of fiber photometry experiments coupled with optogenetic. Our experiments demonstrate that the calcium activity of FSIs differs according to sex and the estrous cycle (**Fig. 20D**), recapitulating our *ex-vivo* electrophysiological data. In

females, the population-level neuronal activity was reduced following optogenetic stimulation only during the proestrus phase. During the other estrous phases, the optogenetic stimulation induced an increase in activity that progressively grew in magnitude following the estrous cycle (**Fig.21**). Those observations are coherent with our ex-vivo electrophysiological data, possibly reflecting cycle-related fluctuations in estradiol and progesterone plasma levels. Although these outcomes clearly emphasize the strong influence of the estrous cycle on thalamic-driven FSI activation, we will strengthen these results by increasing the sample size.

Differences with other studies

We noted that most studies in the literature focus only on changes in circulating plasma levels of sex steroid hormones across the estrous cycle. For this reason, to test whether sex hormones cause sexually dimorphic phenotypes, experiments are often performed on gonadectomized males and females in which bloodborne sex hormones and the female estrous cycle are eliminated. However, sex steroid production is not limited to the periphery, since the brain itself displays the enzymes needed for sex steroid synthesis. The striatum specifically contains the enzyme aromatase, needed for sex hormone synthesis. Moreover, estradiol has been detected in the NAc of ovariectomized rats (*Morissette et al. 1992*), proving that striatal neurons are capable of producing estradiol locally. Thus, although gonadectomy and the consequent elimination of estrus cycle fluctuations in circulating sex hormone levels is sufficient to eliminate sex differences in striatal SPN electrophysiology (*Proano et al., 2020*), local hormone synthesis may play a role in other aspects of striatal function. To recapitulate as closely as possible physiological conditions, we did not gonadectomize mice in our experiments. Our choice comes at the cost of being unable to differentiate the effects of bloodborne and de novo synthesized sex hormones on FSI physiology and thalamic input integration, however, it allows us to better understand the dynamic of striatal changes induced by the local production of sex hormones. Further experiments, outside the scope of this dissertation will be needed to differentiate the effects of locally produced and circulating sex hormones.

An additional source of variability between our results and some of the previous observations is the age of mice, as most of the other previously published works employed prepubertal animals (*Cao et al. 2016*). Prior to puberty, gonadal hormone levels are extremely low in both sexes, with little to no fluctuations in females (*Moraga-Amaro et al., 2018*). Thus, studies performed during this stage could underestimate the potential influence of sex hormones and estrous cycle fluctuations on striatal functions. Moreover, puberty can potentially reorganize neural substrates, including the striatal regions (*Juraska et al., 2013; Staffoend et al., 2014; Kopee et al., 2018*), and introduce a new hormonal dynamic which can alter striatal neuron properties.

We suspect that many other striatal interneuron types and perhaps even **glia**, given their sensitivity to estradiol, can also exhibit differential properties across cycle phases in sexually mature females. For instance, estradiol has been shown to regulate microglial numbers, morphology, and activation in the ventromedial hypothalamus (*Velez/Perez et al., 2020; Liu et al., 2023*). Moreover, circulating estradiol can also stimulate the synthesis of progesterone in adult hypothalamic astrocytes, pointing out a critical role for astrocytes in regulating estrogen-positive feedback at hypothalamo-hypophyseal portal/neurons (*Micevych et al., 2010*). In addition, regulation of glial cell activation toward a neuroprotective phenotype via estradiol is a promising therapeutic approach in Parkinson' disease treatment (*Siani et al., 2017*). Cholinergic interneurons express membrane estrogen receptors and have been implicated in estradiol-induced shifts between hippocampal and striatal-based learning behaviors, suggesting interactions been the estrogen, cholinergic, and dopamine systems (*Euvrard et al., 1979; Davis et al., 2003; Almey et al., 2012*). It should be noted that a thorough analysis of estrogen receptor expression across striatal neurons and interneurons subtypes has not been accomplished.

Material and Methods

Animals

All procedures involving animals were carried out in accordance with the Italian Ministry of Health's directives (D.lgs 26/2014) regulating animal research. Animal experiments were designed following the ARRIVE (Animal Research: Reporting of In Vivo Experiments) guidelines (*Kilkenny et al., 2010*), with a commitment to refinement, reduction, and replacement, minimizing the number of mice. The mouse strain PV-CRE (The Jackson Laboratory) was used in this study. Male and female mice were separately housed 1-5 per cage in a temperature- and humidity-controlled room under a 12:12 h light/dark cycle (lights on at 07:00), with food and water ad libitum.

Estrous cycle assessment

Estrous cycle assessment was performed with a wet mount preparation as previously described (Hubscher et al. 2005). The day of the experiment females (3-4 weeks after the viral injection) were swabbed with potassium phosphate buffer solution and the collected smear was stained with Toluene Blue (2%). Obtained slides were visualized under a microscope to determine estrous cycle stage according to cell morphology. As described in literature (Westwood, 2008), the endocrine events occurring during the murine estrous cycle reflect in changes in vaginal cell topology; thus, estrous stage can be identified on the presence of nucleated epithelial cells, cornified squamous epithelial cells and leukocytes.

Animal surgeries

Viral Injection

Five- to six-week-old mice were anesthetized with a 1.5-2% isoflurane/O2 mixture and fixed in a stereotactic frame (Stoelting). For all injections, the virus volume was delivered at a 0.1 µL/min rate using a syringe (WPI, Nanofil 10 µL) connected to a syringe pump (WPI, UMP3). *Ex-vivo* and *in-vivo* experiments were performed 4 weeks after surgeries to allow viral expression. To specifically target Dorsal Striatum (DS) parvalbumine positive

neurons (FSI) PV-CRE mice were injected with AAV9-flex-td-Tomato (Addgene, volume of 0.5µl per hemisphere) in DLS (relative to Bregma: anteroposterior: -0.4 mm, mediolateral: ±2.2, dorsoventral: -2.3 mm). To optogenetically manipulate PF terminals in the DS, PV-CRE mice were injected with AAV5-Chronos-GFP (Addgene, volume of 0.4µl per hemisphere) in PF (relative to Bregma: anteroposterior: +1.5 mm; mediolateral: +0.78 mm; - dorsoventral:3.5 mm).

Optical fibers implantation

To monitor calcium indicator AAV9-DIO-GCamp8m fluorescence signals, PV-Cre mice were implanted in the DLS with 3 mm long optical fibers (RWD Life Science) (200µm core, NA 0.39; stereotaxic coordinates reported in "*Viral injection*" paragraph) and injected in the Pf with AAV5-hSyn-ChrimsonR-tdTomato (stereotaxic coordinates reported in "*Viral injection*" paragraph).

Ex-vivo electrophysiology

Slice preparation

Mice were anesthetized with isoflurane and decapitated, and their brains were transferred to ice-cold dissecting solution containing 110 mM choline chloride, 2.5 mM KCl, 1.25 mM NaH2PO4, 7 mM MgSO4, 0.5 mM CaCl2, 25 mM NaHCO3, 25 mM D-glucose, 11.6 mM sodium-L-ascorbate and 3.1 mM sodium pyruvate. Dissecting solutions were saturated with 95% O2 and 5% CO2. Horizontal DLS slices (270 µm thick), were obtained using a Vibratome 1000S slicer (Leica), then transferred to artificial cerebrospinal fluid (aCSF) containing 115 mM NaCl, 3.5 mM KCl, 1.2 mM NaH2PO4, 1.3 mM MgCl2, 2 mM CaCl2, 25 mM NaHCO3, and 25 mM D-glucose and aerated with 95% O2 and 5% CO2. Following 15 min of incubation at 32 °C, slices were kept at 22–24 °C. During experiments, slices were continuously superfused with aCSF at a rate of 2 ml/min at 28 °C.

Electrophysiology

For all experiments, whole cell patch-clamp recordings were were made on td-Tomato+ striatal FSIs, which were visualized through the microscope objective (Leica 25x NA 0.95

water immersion objective). During experiments to assess the responsiveness of FSI upon optogenetic stimulation of Pf fibers on *ex-vivo* brain slices patch pipettes (3-4 MΩ) were filled with a solution containing 30 mM KMeSO4, 5 KM 21 KCl, 5 mM NaCl, 10 mM HEPES, 2 mM MgCl2, 0.1 mM EGTA, 0.05 mM CaCl2, 2 mM Na2ATP and 0.4 mM Na3GTP, pH 7.2–7.3 (280–290 mOsm/kg). The GABAA receptor antagonist gabazine (10μM) was present in the bath during the entire duration of the experiment. In a subset of experiments also the vehicle DMSO 0.01% and the estrogen receptor agonist ICI172880 (Fulvestrant, 10μM) were bath-applied. Glutamatergic inputs from thalamus were activated using trains of stimuli at frequency range of 40Hz, and the EPSCs (excitatory post synaptic currents) evoked were recorded from td-Tomato^{+} FSIs. The protocol of stimulation was composed by a presynaptic train (20 sweeps, 3s each) of 10 pulses (1ms duration) delivered with interstimulus intervals that correspond to the stimulation frequency desired, with a holding potential of -70 mV. The stimulus intensity was adjusted to obtain an initial EPSC with an amplitude about -10 to -200 pA. AMPA and NMDA receptor-mediated EPSC were recorded at -70mV and +40mV, respectively. NMDA currents were recorded in presence of the AMPA receptors-antagonist NBQX disodium salt (20μM). During intrinsic properties experiments FSI excitability and rheobase were assessed in current-clamp mode. At least three series of depolarizing and hyperpolarizing current injections (from -100pA to 800pA; delta level 100 pA) were applied to elicit neurons excitability. Recordings lasted 10 sweeps; each sweep consisted in 400ms. The rheobase value for each cell was assessed by injection of a series of positive current steps (from +90pA to +500pA; delta level 20pA); each sweep consisted of 400ms. Cell membrane properties were extracted performing injection of a negative voltage step (-5 mV, 150 ms) from the resting membrane potential in voltage-clamp mode. Electrophysiological experiments were performed in the presence of the GABAA receptor antagonist gabazine (10μM), the NMDA receptor antagonist APV (30μM) and the AMPA receptor antagonist NBQX (20μM). In a subset of experiments also the vehicle DMSO 0.01% and the estrogen receptor agonist ICI172880 (Fulvestrant, 10μM) were bath-applied. Data were excluded when the access resistance (Ra) changed >20%. During electrophysiology experiments, putative FSIs were filled with Neurobiotin (0.5 mg/ml) and slices were subsequently fixed with 4% PFA for immunohystochemical experiments. Data

were acquired using a Multiclamp 700B amplifier controlled by pClamp 10 software (Molecular Device), filtered at 2.4 kHz and sampled at 10 kHz (voltage-clamp), or filtered at 2.4 kHz and sampled at 5 kHz (current-clamp) (Digidata 1322, Molecular Device).

Data Analysis

The action potential firing rate was expressed as the number of spikes per each step of input current. Rheobase, measured in picooamps, is the lowest amplitude of injected positive current needed to produce an initial action potential and was counted considering the input current step that elicit an action potential. Passive membrane properties (membrane capacitance, membrane resistance and time constant of the membrane) were calculated by fitting a single exponential curve to the membrane potential change in response to -5mV hyperpolarizing pulses. For optogenetic experiments, EPSC amplitude was obtained by averaging the mean amplitude of 10 stimuli in 20 consecutive sweeps and measured in picoamps. In pharmacology experiments involving the estrogen receptor blocker, the action potential firing rate, rheobase, passive membrane properties and EPSC amplitude were obtained as described above, and changes were evaluated comparing the pre-condition in DMSO and post pharmacological superfusion.

In-vivo fiber photometry

Calcium activity recording in DLS upon optogenetic stimulation of Pf terminals

Pv-Cre mice were placed in an open field arena where they were free to explore for five consecutive day before the fiber photometry experiments for a total of 15 min. On the sixth day, we performed combined optogenetic and fiber photometry experiments to collect bulk calcium signals from FSI ensembles in freely behaving mice. Prior to fiber photometry recording, a ferrule sleeve was used to connect a matching optic fiber to the implanted fiber in DLS. To optogenetically stimulate Chrimson^{+} Pf terminal in the DLN, a pulse train stimulation (20Hz for 1s, 20ms pulse width) was delivered to the DLN using a 590nm laser with an output power of 1mW/mm^2 measured at the fiber tip. The optogenetic stimulation was delivered as followed: 4 pulse trains with an inter-stimulus interval of 1min. The

calcium fluorescence signal was recorded simultaneously in the DLS using a 470nm laser (a 415nm signal was recorded as isosbestic reference) with an output power of 80-90µW measured at the fiber tip.

Data analysis

Fiber photometry data were analyzed using custom-made python script. Briefly, the fluorescence signals at 470nm (signal) and 415nm (isosbestic) were first lowess smoothed, then the difference over the isosbestic (ΔF/F) was computed. Finally, we expressed the Z-score signal as the ΔF/F normalized according to the baseline. In the optogenetic experiments, we obtained the Z-score time course for each mouse by averaging 4 consecutive optogenetic train stimuli. The A.U.C. values represented the integrated area of the fluorescence signal, analyzed using Origin 9.1 (OriginLab Corporation, MA, USA).

Immunofluorescence

Electrophysiology slices were blocked and permeabilized for 1,5 hour in PBS containing 5% normal goatserum and 0.5% Triton X after which they were incubated for 48 hours at 4 degrees with primary antibodies in PBS containing 1% normal goat serum and 0.5% Triton X. The parvalbumin marker PV was detected with mouse anti-PV (1:1000) antibody. After PBS washes, slices were incubated with Streptavidin for 4 hours to label Neurobiotin. Then, slices were incubated with Alexa-labeled secondary antibodies for 1.5 hours (1:500, Molecular Probes, OR, USA). After incubation with DAPI (1:1000) for 30 minutes at room temperature sections were mounted in ProLongTm Diamond Antifade Mountant (Molecular Probes). Images were acquired with an inverted Leica TCS SP5 AOBS TANDEM confocal microscope.

Drugs

Neurobiotin was purchased from DBA. Triton-X, KMeSO4, KCl, NaCl, HEPES, MgCl2, EGTA, CaCl2, Na2ATP, Na3GTP, choline chloride, NaH2PO4, MgSO4, NaHCO3, D-glucose, sodium-L-ascorbate and sodium pyruvate were purchased from Sigma Aldrich.

Gabazine, APV and NBQX were all purchased by Tocris (United Kingdom) and diluted in water. ICI172880 was purchased by Tocris (United Kingdom) and diluted in DMSO.

Statistic

Appropriate parametric statistics were used to test our hypothesis unless the data did not meet the assumptions of the intended parametric test (normality test). In that case, appropriate nonparametric tests were used. Data were analyzed by one-way repeated measures ANOVA for comparison within a group. Two-way repeated measure or mixed design ANOVA was used in the case comparisons with respectively two independent or dependent factors (GraphPad Prism 7/9 software). Two-group comparisons were performed with t-test, for normally distributed data, or Wilcoxon matched-pairs signed rank test for non-normally distributed data (GraphPad Prism 7 software). Statistical details of experiments are shown in the results, figures, and figure legends. Data are reported as mean ± SEM *$p<0.05$, **$p<0.01$, ***$p<0.001$, ****$p<0.0001$.

Bibliography

Adam EM, Brown EN, Kopell N, McCarthy MM. (2022) Deep brain stimulation in the subthalamic nucleus for Parkinson's disease can restore dynamics of striatal networks. *Epub* 10;119(19):e2120808119. doi:10.1073/pnas.2120808119.

Almey A, Milner TA, Brake WG. (2015) Estrogen receptors in the central nervous system and their implication for dopamine-dependent cognition in females; *Epub* 74:125-38. doi: 10.1016/j.yhbeh.2015.06.010.

Aoki S, Liu AW, Zucca A, Zucca S, Wickens JR. (2015) Role of Striatal Cholinergic Interneurons in Set-Shifting in the Rat. *J Neurosci*. 24;35(25):9424-31. doi: 10.1523/JNEUROSCI.0490-15.2015.

Aranda A, Pascual A. Nuclear hormone receptors and gene expression. (2001) *Physiol Rev* : 81(3):1269-304. doi: 10.1152/physrev.2001.81.3.1269.

Assous M, Tepper JM. Cortical and thalamic inputs exert cell type-specific feedforward inhibition on striatal GABAergic interneurons. (2019) *J Neurosci Res*.;97(12):1491-1502. doi: 10.1002/jnr.24444.

Graveland GA, Williams RS, DiFiglia M. (1985) Evidence for degenerative and regenerative changes in neostriatal spiny neurons in Huntington's disease. *Science*.;227(4688):770-3. doi: 10.1126/science.3155875.

Báez-Mendoza R, Schultz W. (2013) The role of the striatum in social behavior. *Front Neurosci*: 10;7:233. doi: 10.3389/fnins.2013.00233.

Balleine BW, Delgado MR, Hikosaka O. (2007) The role of the dorsal striatum in reward and decision-making. *J Neurosci*. 1;27(31):8161-5. doi: 10.1523/JNEUROSCI.1554-07.2007.

Barth C, Villringer A, Sacher J. (2015) Sex hormones affect neurotransmitters and shape the adult female brain during hormonal transition periods. *Front Neurosci*. doi: 10.3389/fnins.2015.00037.

Basile GA, Bertino S, Bramanti A, Ciurleo R, Anastasi GP, Milardi D, Cacciola A. (2021) Striatal topographical organization: Bridging the gap between molecules, connectivity and behavior. *Eur J Histochem*. 13;65(s1):3284. doi: 10.4081/ejh.2021.3284.

Beatty WW. (1979) Gonadal hormones and sex differences in nonreproductive behaviors in rodents: organizational and activational influences. *Horm Behav*.;12(2):112-63. doi: 10.1016/0018-506x(79)90017-5.

Becker JB, Snyder PJ, Miller MM, Westgate SA, Jenuwine MJ.(1987) The influence of estrous cycle and intrastriatal estradiol on sensorimotor performance in the female rat. *Pharmacol Biochem Behav*.;27(1):53-9. doi: 10.1016/0091-3057(87)90476-x.

Becker JB. (2016) Sex differences in addiction. *Dialogues Clin Neurosci*.;18(4):395-402. doi: 10.31887/DCNS.2016.18.4/jbecker.

Benavidez NL, Bienkowski MS, Zhu M, Garcia LH, Fayzullina M, Gao L, Bowman I, Gou L, Khanjani N, Cotter KR, Korobkova L, Becerra M, Cao C, Song MY, Zhang B, Yamashita S, Tugangui AJ, Zingg B, Rose K, Lo D, Foster NN, Boesen T, Mun HS, Aquino S, Wickersham IR, Ascoli GA, Hintiryan H, Dong HW.(2021) Organization of the inputs and outputs of the mouse superior colliculus. *Nat Commun.* 28;12(1):4004. doi: 10.1038/s41467-021-24241-2.

Berke JD. (2008) Uncoordinated firing rate changes of striatal fast-spiking interneurons during behavioral task performance. *J Neurosci*. 1;28(40):10075-80. doi: 10.1523/JNEUROSCI.2192-08.2008.

Berke JD (2011) . Functional properties of striatal fast-spiking interneurons. *Front Syst Neurosci*. 20;5:45. doi: 10.3389/fnsys.2011.00045.

Berlanga ML, Olsen CM, Chen V, Ikegami A, Herring BE, Duvauchelle CL, Alcantara AA. (2003) Cholinergic interneurons of the nucleus accumbens and dorsal striatum are activated by the self-administration of cocaine. *Neuroscience.*;120(4):1149-56. doi: 10.1016/s0306-4522(03)00378-6.

Bertran-Gonzalez J, Bosch C, Maroteaux M, Matamales M, Hervé D, Valjent E, Girault JA. (2008) Opposing patterns of signaling activation in dopamine D1 and D2 receptor-expressing striatal neurons in response to cocaine and haloperidol. *J Neurosci*.; 28(22):5671-85. doi: 10.1523/JNEUROSCI.1039-08.2008.

Biever A, Valjent E, Puighermanal E. (2015) Ribosomal Protein S6 Phosphorylation in the Nervous System: From Regulation to Function. *Front Mol Neurosci*;8:75. doi: 10.3389/fnmol.2015.00075

Blumenstock S, Dudanova I.(2020) Cortical and Striatal Circuits in Huntington's Disease. *Front Neurosci* 6;14:82. doi: 10.3389/fnins.2020.00082.

Bourque M, Dluzen DE, Di Paolo T. (2011) Male/Female differences in neuroprotection and neuromodulation of brain dopamine. *Front Endocrinol* (Lausanne). 2011 Sep 30;2:35. doi: 10.3389/fendo.2011.00035.

Burke DA, Rotstein HG, Alvarez VA(2017) . Striatal Local Circuitry: A New Framework for Lateral Inhibition. *Neuron*. 11;96(2):267-284. doi: 10.1016/j.neuron.2017.09.019.

Castrioto A, Hulliger S, Poon YY, Lang AE, Moro E. (2010) A survey on the impact of the menstrual cycle on movement disorders severity. *Can J Neurol Sci*;37(4):478-81. doi: 10.1017/s0317167100010490.

Clarke RA, Lee S, Eapen V. (2012) Pathogenetic model for Tourette syndrome delineates overlap with related neurodevelopmental disorders including Autism. *Transl Psychiatry*.;2(9):e158. doi: 10.1038/tp.2012.75. Erratum in: *Transl Psychiatry*. 2012;2:e163.

Corcoran J, Berry A, Hill S. (2015) The lived experience of US parents of children with autism spectrum disorders: a systematic review and meta-synthesis. *J Intellect Disabil*.;19(4):356-66. doi: 10.1177/1744629515577876.

Cora MC, Kooistra L, Travlos G. (2015) Vaginal Cytology of the Laboratory Rat and Mouse: Review and Criteria for the Staging of the Estrous Cycle Using Stained Vaginal Smears. *Toxicol Pathol* ;43(6):776-93. doi: 10.1177/0192623315570339.

Crabtree JW. Functional Diversity of Thalamic Reticular Subnetworks. (2018) *Front Syst Neurosci*.;12:41. doi: 10.3389/fnsys.2018.00041.

Daniel R, Pollmann S. (2014) A universal role of the ventral striatum in reward-based learning: evidence from human studies. *Neurobiol Learn Mem*.;114:90-100. doi: 10.1016/j.nlm.2014.05.002.

Day JJ, Sweatt JD. (2012) Epigenetic treatments for cognitive impairments. *Neuropsychopharmacology*;37(1):247-60. doi: 10.1038/npp.2011.85. Epub 2011 May 18.

DiCarlo GE, Aguilar JI, Matthies HJ, Harrison FE, Bundschuh KE, West A, Hashemi P, Herborg F, Rickhag M, Chen H, Gether U, Wallace MT, Galli A. (2019) Autism-linked dopamine transporter mutation alters striatal dopamine neurotransmission and dopamine-dependent behaviors. *J Clin Invest*.;129(8):3407-3419. doi: 10.1172/JCI127411.

Domonkos E, Hodosy J, Ostatníková D, Celec P. (2018) On the Role of Testosterone in Anxiety-Like Behavior Across Life in Experimental Rodents. *Front Endocrinol (Lausanne)*;9:441. doi: 10.3389/fendo.2018.00441.

Dorris DM, Cao J, Willett JA, Hauser CA, Meitzen J. (2015) Intrinsic excitability varies by sex in prepubertal striatal medium spiny neurons. *J Neurophysiol*.;113(3):720-9. doi: 10.1152/jn.00687.2014.

Epstein J, Pan H, Kocsis JH, Yang Y, Butler T, Chusid J, Hochberg H, Murrough J, Strohmayer E, Stern E, Silbersweig DA. (2006) Lack of ventral striatal response to positive stimuli in depressed versus normal subjects. *Am J Psychiatry*;163(10):1784-90. doi: 10.1176/ajp.2006.163.10.1784.

Fink G, Sumner BE, McQueen JK, Wilson H, Rosie R. (1998) Sex steroid control of mood, mental state and memory. *Clin Exp Pharmacol Physiol*;25(10):764-75. doi: 10.1111/j.1440-1681.1998.tb02151.x.

Foy MR, Akopian G, Thompson RF. (2008) Progesterone regulation of synaptic transmission and plasticity in rodent hippocampus. *Learn Mem*.;15(11):820-2. doi: 10.1101/lm.1124708.

Gagnon D, Petryszyn S, Sanchez MG, Bories C, Beaulieu JM, De Koninck Y, Parent A, Parent M. (2017) Striatal Neurons Expressing D_1 and D_2 Receptors are Morphologically Distinct and Differently Affected by Dopamine Denervation in Mice. *Sci Rep*.;7:41432. doi: 10.1038/srep41432.

Gertler TS, Chan CS, Surmeier DJ. Dichotomous anatomical properties of adult striatal medium spiny neurons. (2008) *J Neurosci* ;28(43):10814-24. doi: 10.1523/JNEUROSCI.2660-08.2008.

Graybiel AM, Grafton ST. (2015) The striatum: where skills and habits meet. *Cold Spring Harb Perspect Biol*.;7(8):a021691. doi: 10.1101/cshperspect.a021691.

Gross KS, Moore KM, Meisel RL, Mermelstein PG. (2018) mGluR5 Mediates Dihydrotestosterone-Induced Nucleus Accumbens Structural Plasticity, but Not Conditioned Reward. *Front Neurosci*;12:855. doi: 10.3389/fnins.2018.00855.

Herrera GM, Nelson MT. Differential regulation of SK and BK channels by Ca(2+) signals from Ca(2+) channels and ryanodine receptors in guinea-pig urinary bladder myocytes. (2022) *J Physiol*.;541(Pt 2):483-92. doi: 10.1113/jphysiol.2002.017707.

Jin X, Costa RM. (2010) Start/stop signals emerge in nigrostriatal circuits during sequence learning. *Nature*.;466(7305):457-62. doi: 10.1038/nature09263.

Johansson Y, Silberberg G. (2020) The Functional Organization of Cortical and Thalamic Inputs onto Five Types of Striatal Neurons Is Determined by Source and Target Cell Identities. *Cell Rep* ;30(4):1178-1194.e3. doi: 10.1016/j.celrep.2019.12.095.

Kelly MJ, Qiu J, Wagner EJ, Rønnekleiv OK. (2002) Rapid effects of estrogen on G protein-coupled receptor activation of potassium channels in the central nervous system (CNS). *J Steroid Biochem Mol Biol*.;83(1-5):187-93. doi: 10.1016/s0960-0760(02)00249-2.

Kelly MJ, Lagrange AH, Wagner EJ, Rønnekleiv OK. (1999) Rapid effects of estrogen to modulate G protein-coupled receptors via activation of protein kinase A and protein kinase C pathways. *Steroids* ;64(1-2):64-75. doi: 10.1016/s0039-128x(98)00095-6.

Kloner RA, Carson C 3rd, Dobs A, Kopecky S, Mohler ER 3rd. (2016) Testosterone and Cardiovascular Disease. *J Am Coll Cardiol* ;67(5):545-57. doi: 10.1016/j.jacc.2015.12.005.

Kreitzer AC, Malenka RC. (2008) Striatal plasticity and basal ganglia circuit function. *Neuron*. 60(4):543-54. doi: 10.1016/j.neuron.2008.11.005.

Krentzel AA, Meitzen J. (2018) Biological Sex, Estradiol and Striatal Medium Spiny Neuron Physiology: A Mini-Review. *Front Cell Neurosci*. 12:492. doi: 10.3389/fncel.2018.00492.

Krentzel AA, Willett JA, Johnson AG, Meitzen J. (2021) Estrogen receptor alpha, G-protein coupled estrogen receptor 1, and aromatase: Developmental, sex, and region-specific differences across the rat caudate-putamen, nucleus accumbens core and shell. *J Comp Neurol*. 529(4):786-801. doi: 10.1002/cne.24978.

Kundakovic M, Rocks D. (2022) Sex hormone fluctuation and increased female risk for depression and anxiety disorders: From clinical evidence to molecular mechanisms. *Front Neuroendocrinol*. 66:101010. doi: 10.1016/j.yfrne.2022.101010.

Kuo HY, Liu FC. (2020) Pathological alterations in striatal compartments in the human brain of autism spectrum disorder. *Mol Brain*. 13(1):83. doi: 10.1186/s13041-020-00624-2.

Lovick TA, Zangrossi H Jr. (2021) Effect of Estrous Cycle on Behavior of Females in Rodent Tests of Anxiety. *Front Psychiatry*. 12:711065. doi: 10.3389/fpsyt.2021.711065.

Luoma JI, Kelley BG, Mermelstein PG. (2011) Progesterone inhibition of voltage-gated calcium channels is a potential neuroprotective mechanism against excitotoxicity. *Steroids*. 76(9):845-55. doi: 10.1016/j.steroids.2011.02.013.

McArthur S, Gillies GE. (2011) Peripheral vs. Central Sex Steroid Hormones in Experimental Parkinson's Disease. *Front Endocrinol (Lausanne).* 2:82. doi: 10.3389/fendo.2011.00082.

McLean AC, Valenzuela N, Fai S, Bennett SA. (2012) Performing vaginal lavage, crystal violet staining, and vaginal cytological evaluation for mouse estrous cycle staging identification. *J Vis Exp*. (67):e4389. doi: 10.3791/4389.

Meitzen J, Meisel RL, Mermelstein PG. (2018) Sex Differences and the Effects of Estradiol on Striatal Function. *Curr Opin Behav Sci*. 23:42-48. doi: 10.1016/j.cobeha.2018.03.007.

Meitzen J, Pflepsen KR, Stern CM, Meisel RL, Mermelstein PG. (2011) Measurements of neuron soma size and density in rat dorsal striatum, nucleus accumbens core and nucleus accumbens shell: differences between striatal region and brain hemisphere, but not sex. *Neurosci Lett*. 487(2):177-81. doi: 10.1016/j.neulet.2010.10.017.

Moraga-Amaro R, van Waarde A, Doorduin J, de Vries EFJ. (2018) Sex steroid hormones and brain function: PET imaging as a tool for research. *J Neuroendocrinol*. 30(2):e12565. doi: 10.1111/jne.12565.

Nillni YI, Toufexis DJ, Rohan KJ. (2011) Anxiety sensitivity, the menstrual cycle, and panic disorder: a putative neuroendocrine and psychological interaction. *Clin Psychol Rev*. 31(7):1183-91. doi: 10.1016/j.cpr.2011.07.006.

Nisenbaum ES, Wilson CJ. (1995) Potassium currents responsible for inward and outward rectification in rat neostriatal spiny projection neurons. *J Neurosci*. 15(6):4449-63. doi: 10.1523/JNEUROSCI.15-06-04449.1995.

North KC, Shaw AA, Bukiya AN, Dopico AM. (2023) Progesterone activation of β_1-containing BK channels involves two binding sites. *Nat Commun*. 14(1):7248. doi: 10.1038/s41467-023-42827-w.

O'Lone R, Frith MC, Karlsson EK, Hansen U. (2004) Genomic targets of nuclear estrogen receptors. *Mol Endocrinol*. 18(8):1859-75. doi: 10.1210/me.2003-0044.

Orduz D, Bischop DP, Schwaller B, Schiffmann SN, Gall D. (2013) Parvalbumin tunes spike-timing and efferent short-term plasticity in striatal fast spiking interneurons. *J Physiol*. 591(13):3215-32. doi: 10.1113/jphysiol.2012.250795.

Palmiter RD. (2008) Dopamine signaling in the dorsal striatum is essential for motivated behaviors: lessons from dopamine-deficient mice. *Ann N Y Acad Sci*. 1129:35-46. doi: 10.1196/annals.1417.003.

Patel HK, Bihani T. (2017) Selective estrogen receptor modulators (SERMs) and selective estrogen receptor degraders (SERDs) in cancer treatment. *Pharmacol Ther*. 186:1-24. doi: 10.1016/j.pharmthera.2017.12.012.

Pickrell AM, Pinto M, Hida A, Moraes CT. (2011) Striatal dysfunctions associated with mitochondrial DNA damage in dopaminergic neurons in a mouse model of Parkinson's disease. *J Neurosci*. 31(48):17649-58. doi: 10.1523/JNEUROSCI.4871-11.2011.

Plant TM, Marshall GR. (2011) The functional significance of FSH in spermatogenesis and the control of its secretion in male primates. *Endocr Rev*. 22(6):764-86. doi: 10.1210/edrv.22.6.0446.

Proaño SB, Krentzel AA, Meitzen J. (2020) Differential and synergistic roles of 17β-estradiol and progesterone in modulating adult female rat nucleus accumbens core medium spiny neuron electrophysiology. *J Neurophysiol*. 123(6):2390-2405. doi: 10.1152/jn.00157.2020.

Quinlan MG, Almey A, Caissie M, LaChappelle I, Radiotis G, Brake WG. (2013) Estradiol and striatal dopamine receptor antagonism influence memory system bias in the female rat. *Neurobiol Learn Mem.* 106:221-9. doi: 10.1016/j.nlm.2013.08.018.

Rapanelli M, Frick LR, Xu M, Groman SM, Jindachomthong K, Tamamaki N, Tanahira C, Taylor JR, Pittenger C. (2017) Targeted Interneuron Depletion in the Dorsal Striatum Produces Autism-like Behavioral Abnormalities in Male but Not Female Mice. *Biol Psychiatry*. 82(3):194-203. doi: 10.1016/j.biopsych.2017.01.020.

Schneider AE, Kárpáti E, Schuszter K, Tóth EA, Kiss E, Kulcsár M, László G, Matko J. (2014) A dynamic network of estrogen receptors in murine lymphocytes: fine-tuning the immune response. *J Leukoc Biol*. 96(5):857-72. doi: 10.1189/jlb.2A0214-080RR.

Sherman BM, Korenman SG. (1975) Hormonal characteristics of the human menstrual cycle throughout reproductive life. *J Clin Invest*. 55(4):699-706. doi: 10.1172/JCI107979.

Shu SY, Jiang G, Zheng Z, Ma L, Wang B, Zeng Q, Li H, Tan S, Liu B, Chan WY, Wu S, Zhu C, Li C, Wang P, Wu JY. (2019) A New Neural Pathway from the Ventral Striatum to the Nucleus Basalis of Meynert with Functional Implication to Learning and Memory. *Mol Neurobiol*. 56(10):7222-7233. doi: 10.1007/s12035-019-1588-0.

Simpson EH, Kellendonk C, Kandel E. (2010) A possible role for the striatum in the pathogenesis of the cognitive symptoms of schizophrenia. *Neuron*. 65(5):585-96. doi: 10.1016/j.neuron.2010.02.014.

Smith Y, Galvan A, Ellender TJ, Doig N, Villalba RM, Huerta-Ocampo I, Wichmann T, Bolam JP. (2014) The thalamostriatal system in normal and diseased states. *Front Syst Neurosci*. 8:5. doi: 10.3389/fnsys.2014.00005.

Stefaniak M, Dmoch-Gajzlerska E, Jankowska K, Rogowski A, Kajdy A, Maksym RB. (2023) Progesterone and Its Metabolites Play a Beneficial Role in Affect Regulation in the Female Brain. *Pharmaceuticals (Basel).* 16(4):520. doi: 10.3390/ph16040520.

Studelska DR, Beatty WW. (1978) Open-field and avoidance behavior after neostriatal lesions in male and female rats. *J Comp Physiol Psychol*. 92(2):297-311. doi: 10.1037/h0077463.

Thomas MP, Potter BV. (2013) The structural biology of oestrogen metabolism. *J Steroid Biochem Mol Biol*. 137:27-49. doi: 10.1016/j.jsbmb.2012.12.014.

Tobiansky DJ, Wallin-Miller KG, Floresco SB, Wood RI, Soma KK. (2018) Androgen Regulation of the Mesocorticolimbic System and Executive Function. *Front Endocrinol (Lausanne)*. 9:279. doi: 10.3389/fendo.2018.00279.

Uchimura N, Cherubini E, North RA. (1989) Inward rectification in rat nucleus accumbens neurons. *J Neurophysiol*. 62(6):1280-6. doi: 10.1152/jn.1989.62.6.1280.

Vegeto E, Villa A, Della Torre S, Crippa V, Rusmini P, Cristofani R, Galbiati M, Maggi A, Poletti A. (2020) The Role of Sex and Sex Hormones in Neurodegenerative Diseases. *Endocr Rev*. 41(2):273–319. doi: 10.1210/endrev/bnz005.

Vergara C, Latorre R, Marrion NV, Adelman JP. (1998) Calcium-activated potassium channels. *Curr Opin Neurobiol*. 8(3):321-9. doi: 10.1016/s0959-4388(98)80056-1.

Wong JE, Cao J, Dorris DM, Meitzen J. (2016) Genetic sex and the volumes of the caudate-putamen, nucleus accumbens core and shell: original data and a review. *Brain Struct Funct*. 221(8):4257-4267. doi: 10.1007/s00429-015-1158-9.

Yin HH. (2010) The sensorimotor striatum is necessary for serial order learning. *J Neurosci.* 30(44):14719-23. doi: 10.1523/JNEUROSCI.3989-10.2010.

Zheng Q, Ba X, Wang Q, Cheng J, Nan J, He T. (2023) Functional differentiation of the dorsal striatum: a coordinate-based neuroimaging meta-analysis. *Quant Imaging Med Surg.* 13(1):471-488. doi: 10.21037/qims-22-133. Epub 2022 Sep 14.